# Magnetism and superconductivity in strongly correlated systems

Yu. A. Izyumov

*Institute of Metal Physics, Ural Branch of the Academy of Sciences of the USSR, Ekaterinburg*
(Submitted 17 July 1991)
Usp. Fiz. Nauk **161**, 1–46 (November 1991)

Current ideas on the interaction between magnetic and superconducting states in strongly magnetized systems are discussed in terms of the Hubbard model and its limiting case in the form of the $t-J$ model. Two approaches to the problem are compared, namely, those of weak and strong Coulomb repulsion, i.e., $U \ll W$ and $U \gg W$, respectively, where $U$ is the repulsion and $W$ the electronic band width. The dynamic magnetic susceptibility of the system is analyzed in both cases, and different types of magnetic instability are identified. Spin fluctuations that grow near the instability boundaries of the paramagnetic phase give rise to Cooper instability. The role of longitudinal and transverse spin fluctuations in the evolution of the superconducting state in a magnetically ordered phase is also investigated. Particular attention is devoted to the two-dimensional model near half-filling. Analytic studies based on the generalized random phase approximation are presented. In addition, a detailed review is given of numerical calculations that involve a single hole in the antiferromagnetic phase and are based on the Monte Carlo method and the exact diagonalization of small clusters. The problem of two interacting holes is also examined. Such studies may provide the conceptual basis for magnetic (correlational) mechanisms of high-$T_c$ superconductivity in copper oxide compounds.

## 1. INTRODUCTION TO THE PROBLEM

### 1.1. Fundamental models in the theory of strongly correlated systems

The media in which the characteristic Coulomb interaction energy of electrons is greater than or of the order of the bandwidth are called strongly correlated systems. They have attracted exceptional interest in recent years in connection with searches for nonphonon mechanisms in high-$T_c$ superconductors such as the copper cuprates. It has become clear from current experimental data and *ab initio* calculations of the band spectrum that these materials belong to the class of strongly correlated systems. This correlation is indicated by the proximity of superconducting compositions to the metal-insulator and antiferromagnetic transitions, and by the presence of localized magnetic moments in copper. There are quite a few hypotheses that associate high $T_c$ with manifestations of strong electronic correlation.

It is well known that strongly correlated systems have a tendency toward magnetic and superconducting ordering, so that the superconductivity problem for such systems must be considered in the context of studies of magnetic states. It was shown well before the discovery of high-$T_c$ superconductivity that the indirect interaction between electrons near a ferromagnetic instability in a metal gives rise to a repulsion in the singlet channel and to an attraction in the triplet channel.[1] Much later it was shown[2] that the potential experienced by electrons in a singlet pair near an antiferromagnetic instability is also repulsive although this may be accompanied by the onset of superconductivity with anisotropic d-wave order parameter. This type of behavior of itinerant magnets in the paramagnetic phase with respect to Cooper pairing is fully consistent with the well-established fact that the interaction between electrons via magnetic fluctuations (spin waves) in a magnetically ordered state is repulsive in the singlet channel and attractive in the triplet channel.[3,4]

The above results[1,2] were obtained for systems with weak Coulomb interactions. The situation is much more complicated in the case of strongly correlated systems because localized magnetic moments that can give rise to pair breaking[5] can then appear in the system for a certain particular electron concentration. The connection between magnetic and superconducting states can be investigated most completely in terms of the Hubbard model.[6]

The Hamiltonian for the Hubbard model contains only two parameters, namely, the transition matrix element $t$ between the nearest-neighbor sites and the Coulomb repulsion parameter $U$ of electrons on a given site. In the second quantization representation, the Hamiltonian can be expressed in terms of the Fermi annihilation and creation operators $c_{i\sigma}$ and $c_{i\sigma}^{+}$ of an electron on site $i$ with spin $\sigma$:

$$\mathcal{H} = -t\sum_{i,j,\sigma} c_{i\sigma}^{+}c_{j\sigma} + U\sum_{i} n_{i\uparrow}n_{i\downarrow}; \tag{1.1}$$

where $n_{i\sigma} = c_{i\sigma}^{+}c_{i\sigma}$ is the number of electrons with given spin $\sigma$ on a given site.

The system as a whole is characterized by a further parameter, namely, the electron concentration $n$ (number of electrons per site) which ranges from 0 to 2. Half-filling ($n = 1$) is a special case because an insulating state with

 0038-5670/91/110935-23$01.00  

long-range magnetic order can occur for certain ratios of $t$ and $U$. It is convenient to take the bandwidth $W = 2zt$ as the parameter characterizing the first (band) term in the Hamiltonian, where $z$ is the number of nearest neighbors. The most interesting parameter range in which one finds magnetic ordering, the metal-insulator phase transition, and so on is the intermediate region $U \sim W$ which is relatively inaccessible to analytic investigation. It is therefore usual to examine two limiting cases, namely, $U \ll W$, which corresponds to the usual Fermi liquid, and $U \gg W$, which corresponds to a strongly-correlated system. A perturbation theory in the appropriate parameter can be developed for each of these limits. The usual Fermi operator technique is used for the weak Coulomb interaction, but perturbation theory is not as trivial in the opposite limit (see, for example, Ref. 7). Since Hubbard's work, the single-site energy is treated in this case as the zero-order approximation and the kinetic term is regarded as a perturbation.

Thus, when $U \ll W$, one starts with the basis of itinerant (band) electronic states whereas for $U \gg W$ the basis of localized states is employed. In the intermediate region, the system exhibits features of both bases, which are analogous to the usual quantum-mechanical wave-particle dualism of micro-objects. Hubbard has put forward an interpolation scheme for the description of the intermediate region, but this is found to be too approximate for the description of cooperative phenomena such as the phase transition to a magnetic, superconducting, or insulating state. Regular perturbation theory in the parameter $U/W$ or $W/U$, followed by extrapolation to $U \sim W$, is therefore preferable. Indeed, this is the approach adopted by most researchers motivated by the idea of nonphonon mechanisms for high-$T_c$ superconductivity.

In the case of strongly correlated systems ($U \gg W$), it is convenient to start with an effective Hamiltonian and not the original Hamiltonian (1.1). Excluding states with two electrons per site, i.e., 'pairs', we can show that in second-order perturbation theory the Hamiltonian corresponds to the so-called $t-J$ model[8,9]

$$\mathcal{H} = -t\sum_{i,j,\sigma}(1-n_{i,-\sigma})c_{i\sigma}^{+}c_{j\sigma}(1-n_{j,-\sigma}) + J\sum_{i,j}(\mathbf{S}_i\mathbf{S}_j - \tfrac{1}{4}n_in_j); \tag{1.2}$$

where $S_i$ is the electron spin operator, $n_i = \Sigma_\sigma n_{i\sigma}$ is the operator representing the number of electrons per site $i$, and $J = 4t^2/U$ is the effective exchange integral between nearest neighbors. The kinetic term acquires factors of the form $(1-n_{i,-\sigma})$ which prevents electrons from reaching sites that are already occupied. The kinetic term vanishes in the case of half-filling, and the Hamiltonian $\mathcal{H}$ reduces to the Hamiltonian for the Heisenberg antiferromagnet with spin $S = 1/2$. It is clear that this is an insulating state.

Thus, different models with Hamiltonians (1.1) and (1.2) must be used for weak and limiting strong Coulomb interactions, respectively. The same statistical mechanics problem must nevertheless be solved in both cases, e.g., we have to construct the diagram of state on the $(t/U,n)$ plane or, in a more complete form, within the volume $(t/U,n,T)$. In this review, we shall confine ourselves to a part of the general problem, namely, the magnetic and superconducting phases in the itinerant model and to the interrelation between them.

The problem has two aspects, namely, a general aspect that involves the examination of the three-dimensional model in a wide range of electron concentrations, and a special aspect that covers known high-$T_c$ superconductors and involves studies of the two-dimensional model near half-filling. We shall try to examine both these aspects, but will concentrate our attention on the two-dimensional Hubbard model near half-filling. Before we turn to a rigorous discussion of this problem, we present some qualitative ideas on the behavior of holes implanted in an antiferromagnetic lattice at half-filling.[10,11]

### 1.2. Qualitative description of the motion of a hole in a ferromagnetic matrix

Simple considerations suggest that holes can form a bound state in the antiferromagnetic phase near half-filling. Figure 1 shows two configurations containing two holes. In one case, the holes are nearest neighbors whereas in the other they are a certain distance apart. It is clear that the separation of holes produces a sequence of overturned spins that requires an energy proportional to the length of the sequence, i.e., the separation between the holes. It follows that the magnetic order gives rise to an effective hole interaction potential that is responsible for the confinement of the holes. At the same time the hole pair can move freely through the lattice without losing energy by deforming the magnetic structure.

If we wish to model this potential, we must remember that the $t-J$ model involves two time scales, namely, $\tau_h$ which is a measure of the time spent by a hole on a site and $\tau_m$ which is the lifetime of a spin fluctuation. These two parameters are given by

$$\tau_h \sim \hbar/t, \quad \tau_m \sim \hbar/4t^2/U. \tag{1.3}$$

When $U \gg t$, we have $\tau_m \gg \tau_h$, so that the motion of the hole is fast in comparison with the fluctuation relaxation time. This means that a moving hole produces a sequence of overturned spins over a length $l \sim \tau_m v_F$ where $v_F$ is the velocity on the Fermi surface. The second hole (with the opposite spin) then experiences an attractive potential $v(r)$ that rises linearly over a segment of length $l$. This potential can be approximately represented by

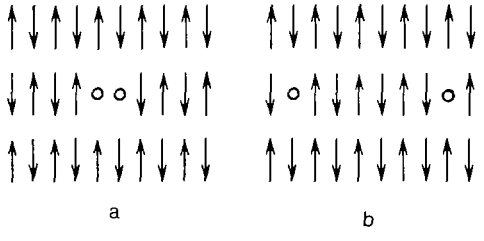


FIG. 1. Spin configurations containing two holes: a–nearest neighbors, b–holes separated by a certain distance.

$$v(r) = \frac{4t^2}{Ua}(r-l), \quad r < l, \qquad = 0, \quad r > l; \tag{1.4}$$

where $a$ is the lattice constant. Of course, the total effective potential must include the radial centrifugal potential

$$v_l(r) \sim \frac{l(l+1)}{r^2}t,$$

where $l$ is the orbital angular momentum of the particle pair. The total potential $v_{\text{eff}}(r) = v(r) + v_l(r)$ is such that a bound state, namely, a Cooper pair, can be formed in the potential. Since, for a singlet state, the orbital part must be an even function, $l$ can correspond to a s-wave state or a d-wave state. We choose the latter because the wave function of the pair then vanishes at $r = 0$, which is in agreement with the fact that two holes cannot occupy the same site.

Despite its primitive character, the above model (or, more precisely, heuristic) approach does describe the overall evolution of the superconducting state in the $t - J$ model. In particular, it outlines the necessity for the close coupling of charge and magnetic degrees of freedom, the special role of the d-wave symmetry of the superconducting order parameter, and the importance of antiferromagnetic ordering. The theory of superconductivity based on the $t - J$ model must be constructed with allowance for these trends and must thus be freed from two coarse asumptions, namely, the *ad hoc* introduction of a pairing potential and the Ising-like antiferromagnetic state. The inclusion of transverse spin components in the analysis extends the basis of spin configurations that must be introduced to describe the perturbation of magnetic order by the moving hole.

In any search for possible pairing mechanisms for real high-$T_c$ materials, we must concentrate our attention on the properties of the two-dimensional $t - J$ model near half-filling (low hole concentration $n_h$). In this situation, we know the ground state of the system that is taken as the zero-order approximation: it is the antiferromagnetic insulator. An individual hole is found to be localized in this system as can be seen from Fig. 1. Several theoretical problems arise at this point, the most important of which are as follows:

(1) How (i.e., for which hole concentration) does metallization of the system occur?

(2) What is the dynamic character of a hole in the form of a quasiparticle with a cloud of magnetic-structure deformation (magnetic polaron)?

(3) What is the lifetime of this quasiparticle, and can the metallized hole collective be described by the Fermi liquid picture?

These are, of course, problems encountered in the description of the normal state of a metal. The second level of problems is concerned with the onset of superconductivity and can be reduced to the problem of a bound state of holes and the evaluation of $T_c$.

### 1.3. Two approaches to the problem of strongly correlated systems

We have thus shown that the most interesting parameter range $U \sim W$ can be approached in two ways, namely, either via perturbation theory in the small parameter $U/W$, using the Hubbard model with the Hamiltonian (1.1), or via the $t - J$ model in which the opposite small parameter $W/U$ has already been used. Accordingly, our review consists of two parts. The first part deals with the idea of an itinerant magnet in which the antiferromagnetic state arises near band half-filling as a result of the nesting of the Fermi surface (the dimension $D = 3$ or 2 does not then have any fundamental significance). In the random-phase approximation (RPA), we investigate the interaction between electrons via spin fluctuations in the paramagnetic phase of a metal near the antiferromagnetic instability in the general case, and in the antiferromagnetic phase in the two-dimensional system near half-filling. The RPA approximation, and also numerical methods, are used to investigate the quasiparticle lifetime, and it is shown that the Fermi liquid picture of carriers remains valid near band half-filling up to $U \sim W$.

The other part of our review is concerned with the opposite limit, namely, that of strongly correlated systems within the framework of the $t - J$ model. As in Part I, here we investigate the interaction of electrons via spin fluctuations in the paramagnetic phase near the antiferromagnetic instability, using the generalized random phase approximation GRPA.[12] However, most of our material refers to the problem of holes in the two-dimensional $t - J$ model near half-filling. This problem is much more complicated for the $t - J$ model than the analogous problem in the case of the weak Coulomb interaction. One of the basic questions is the ground state of the two-dimensional $t - J$ model at half-filling. Here, we shall confine our attention to only one line of investigation in which it is assumed that a Néel antiferromagnetic state exists. However, there is the alternative Anderson hypothesis[13] of a new type of ground state, i.e., that of resonating valence bonds (RVB). This is now an enormous (and independent) field of research that is close to the problem of anion superconductivity.[14] It will require a separate review.

Copper-oxide cuprates constitute a separate subject in which the electron mechanisms of high-$T_c$ superconductivity in real media are discussed. Any analysis of correlation effects, based on the nondegenerate single-band Hubbard model and its derivative, i.e., the $t - J$ model, can only be conceptual in character. Extended Hubbard models that take into account at least two electron bands (genetically related to the d-wave electrons of copper and the p-wave electrons of oxygen) are used for real high-$T_c$ materials and take into account the degeneracy of these electron states, the symmetry of the lattice, and the Coulomb interactions on neighboring sites. This gives rise to a large number of variants with different ratios of the numerous parameters that define the physical content of the different models. The discussion of these models in the context of experimental data and the electronic structure of copper cuprates can also be the subject of a separate review.

A few years ago we published in this journal a review of the magnetic aspect of the high-$T_c$ problem[15] that covered both experimental data and the corresponding theoretical approaches. In the three years since that publication, the subject has developed along three lines, one of which is covered in this review. The other two (the RVB state and expanded models) will also require a systematic presentation and a critical analysis. These three directions constitute the modern magnetic aspect of high-$T_c$ superconductivity.

## I. APPROACH FROM THE SIDE OF WEAK COULOMB INTERACTION

## 2. TYPES OF INSTABILITY IN THE NORMAL PARAMAGNETIC PHASE OF A METAL

### 2.1. Instability with respect to the formation of a spin density wave

Under certain specific conditions, a weak Coulomb repulsion on a site ($U \ll W$) can give rise to a magnetically-ordered state. The possible types of magnetic order are determined by the properties of the dynamic susceptibility $\chi(\mathbf{q},\omega)$ where $\mathbf{q}$ is the wave vector and $\omega$ the frequency. For the paramagnetic phase of a metal, the random phase approximation (RPA) can be expressed in terms of the dynamic susceptibility $\chi_0(\mathbf{q},\omega)$ of free electrons[16]

$$\chi(\mathbf{q},\omega) = \frac{\chi_0(\mathbf{q},\omega)}{1 - U\chi_0(\mathbf{q},\omega)}, \tag{2.1}$$

where

$$\chi_0(\mathbf{q},\omega) = \frac{1}{N}\sum_{\mathbf{k}} \frac{f(\varepsilon_{\mathbf{k}}) - f(\varepsilon_{\mathbf{k}+\mathbf{q}})}{\omega + \varepsilon_{\mathbf{k}+\mathbf{q}} - \varepsilon_{\mathbf{k}} + i\delta}, \tag{2.2}$$

and $f(\varepsilon_{\mathbf{k}})$ is the Fermi distribution function.

Two types of instability follow from (2.1) in the static limit. One of them is the instability with respect to the formation of a homogeneous ferromagnetic state. Actually, it follows from (2.2) that $\chi_0(\mathbf{q},0)$ is equal to the density of states $\rho(\mu)$ on the Fermi surface, so that the magnetic susceptibility diverges as $q \to 0$ and the Stoner factor vanishes: $1 - U\rho(\mu) = 0$.

The other instability arises when there is a nesting of the Fermi surface with wave vector $\mathbf{Q}$:

$$\varepsilon_{\mathbf{k}+\mathbf{Q}} - \mu = -(\varepsilon_{\mathbf{k}} - \mu). \tag{2.3}$$

We then have $\chi_0(\mathbf{Q},0) \approx \rho(\mu)\ln(W/T)$ and $1 - U\chi_0(\mathbf{Q},0) = 0$:

$$T_{\mathrm{m}} \approx W\exp\left(-\frac{1}{U\rho(\mu)}\right), \tag{2.4}$$

defines the magnetic transition point or the chemical potential $\mu$ for $T = 0$ for which a spin-density wave (SDW) state with wave vector $\mathbf{k}_0 = \mathbf{Q}$ appears.

Thus, magnetic ordering will appear in the system either if the Coulomb repulsion is strong enough or nesting occurs on the Fermi surface. We shall assume that nesting occurs, so that a SDW state is produced in a certain region of the phase plane $(T,\mu)$ or $(T,n)$, or for $T = 0$ on the plane of the parameters of the system. A sharp increase in magnetic-order fluctuations arises near the boundary of these states. These fluctuations convey the indirect interaction between electrons and, possibly, give rise to another type of instability, namely, instability with respect to the formation of a condensate of Cooper pairs. Let us examine this problem in greater detail.

### 2.2. Instability in the Cooper channel

To calculate the electron pairing potentials, we start by recalling the graphical interpretation of magnetic susceptibility (2.1). This classical result is represented by the following sum of loop diagrams:[17]

$\chi(q) =$  (2.5)

where the solid line with a black or white arrow represents the electron Green's function (the color of the arrow represents the electron spin) and a broken line represents Coulomb repulsion. The electron Green's function

$$G_\sigma(\mathbf{k},\tau) = -\langle T c_{\mathbf{k}\sigma}(\tau) c^+_{\mathbf{k}\sigma}(0)\rangle \tag{2.6}$$

is the standard Matsubara Green's function[18] with imaginary time $\tau$. In the zero-order approximation,

$$G^0_\sigma(k) = \frac{1}{i\omega_n - \varepsilon_{\mathbf{k}} + \mu}, \tag{2.7}$$

where $k = (\mathbf{k}, i\omega_n)$ is the four-momentum with an imaginary fourth component.

In the zero-order approximation in $U$, the magnetic susceptibility is given by

$$\chi_0(q) = \text{ 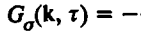 } = \sum_k G^0_\uparrow(k-q)G^0_\downarrow(k), \tag{2.8}$$

which after analytic continuation $i\omega_n \to \omega + i\delta$ leads to the well-known expression (2.2).

The infinite series (2.5) includes dynamic magnetic fluctuations in the system, generated by electron-hole pairs. The effective interaction between electrons in the singlet $V^s$ and triplet $V^t$ channels can be readily expressed in these terms, using the following definitions:[2]

$V^s_{\parallel} =$ 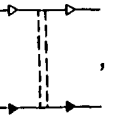 , $V^s_{\perp} =$ 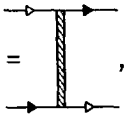 , $V^t =$ 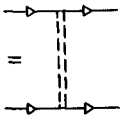 ; (2.9)

where the double dashed lines represent infinite series with even and odd number of loops:

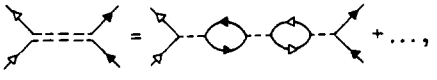 (2.10)

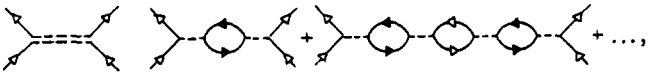 (2.11)

and the dashed vertex part represents the infinite series of antiparallel ladders:

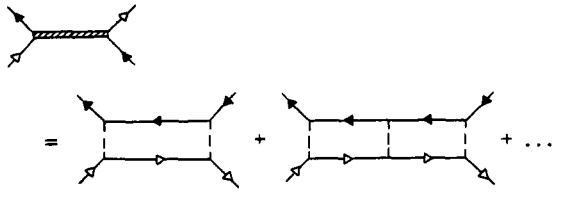 (2.12)

In the Cooper channel (ingoing particle momenta $k$ and $-k$; outgoing momenta $k'$ and $-k'$), the interaction ma-

trix elements $V^s = V_\parallel^s + V_\perp^s$ and $V^t$ in the singlet and triplet states are obviously given by[2]

$$V^s(k, k') = \frac{U}{1 - U^2\chi_0^2(k' - k)} + \frac{U^2\chi_0(k' + k)}{1 - U\chi_0(k' + k)}, \quad (2.13)$$

$$V^t(k, k') = -\frac{U^2\chi_0(k' - k)}{1 - U^2\chi_0^2(k' - k)}. \quad (2.14)$$

We now construct the equation for the vertex part in the Cooper channel. For example, for the singlet state, this has the standard form[18]

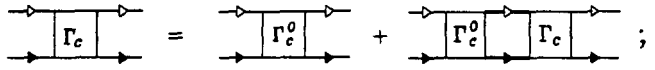


(2.15)

where $\Gamma_c^0$ is the effective interaction $V^s$ defined by the graphical series (2.10) and (2.12) or the analytic expression (2.13). Equation (2.15) without the inhomogeneous term is the linearized equation for the superconducting order parameter and can be used to determine $T_c$. In strong coupling theory, the intermediate Green's functions in (2.15) must be taken to be the renormalized Green's functions with the self-energy part

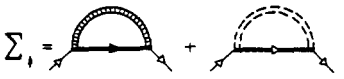


(2.16)

which is obtained by the closure of the intermediate lines in the graphical expressions (2.9) for $V_\parallel^s$ and $V^t$.

Equations (2.15) and (2.16) form a closed set of equations for $\Gamma_c$ and $\Sigma$. As usual, it is convenient to introduce the two quantities $\varphi(k)$ and $Z(k)$. The former is determined by the vertex $\Gamma_c$ for zero total momentum

$$\Gamma_c(k, q - k; q - k', k')\big|_{q=0} \equiv \varphi(k) = \varphi(\mathbf{k}, i\omega_n), \quad (2.17)$$

and the latter is given by the expression for the renormalized Green's function

$$G(k) = (i\omega_n Z(k) - E(\mathbf{k}))^{-1}, \quad (2.18)$$

where $E(\mathbf{k}) = \varepsilon_\mathbf{k} - \mu$ is the energy of the electron measured from the chemical potential. This leads to the following set of coupled equations for $\varphi(k)$ and $Z(k)$:

$$i\omega_n(1 - Z(k)) = \frac{T}{N}\sum_{\mathbf{k}',n'} V_Z(\mathbf{k}\mathbf{k}', i\omega_n - i\omega_{n'})\frac{i\omega_{n'}Z(k')}{(i\omega_{n'}Z(k'))^2 - E^2(\mathbf{k}')}, \quad (2.19)$$

$$\varphi(k) = -\frac{T}{N}\sum_{\mathbf{k}',n'} V(\mathbf{k}\mathbf{k}', i\omega_n - i\omega_{n'})\frac{\varphi(k')}{\left(i\omega_{n'}Z(k')\right)^2 - E^2(\mathbf{k}')}; \quad (2.20)$$

where the matrix elements $V_Z$ and $V$ are given by

$$V(\mathbf{k}\mathbf{k}', i\omega_n - i\omega_{n'}) = -\frac{U}{1 - U^2\chi_0^2(k' - k)} - \frac{U^2\chi_0(k' - k)}{1 - U\chi_0(k' - k)}, \quad (2.21)$$

$$V_Z(\mathbf{k}\mathbf{k}', i\omega_n - i\omega_{n'}) = \frac{U^3\chi_0^2(k' - k)}{1 - U\chi_0(k' - k)} + \frac{U^2\chi_0(k' - k)}{1 - U^2\chi_0^2(k' - k)}. \quad (2.22)$$

Equations (2.19) and (2.20) have the standard form of the equations of the theory of superconductors with strong coupling.[19] The equation for $\varphi(k)$ has a solution for $T_c$ if the matrix element $V$ is positive, which corresponds to attraction. However, it is clear from (2.21) that $V$ is in fact negative because both terms are proportional to the magnetic susceptibility which should be positive in the paramagnetic phase. It follows that the interaction between electrons via magnetic fluctuations is repulsive in the singlet channel, in accordance with the well-known result that the interactions between electrons in this channel via spin waves in the magnetically ordered phase is repulsive.[3]

Despite the repulsive character of the effective interaction (2.21), Cooper pairing is nevertheless possible for an anisotropic superconducting order parameter if the system exhibits antiferromagnetic instability.[2] If we apply the standard treatment to (2.19) and (2.20) in the spirit of the intermediate coupling approximation, we can seek the solution of the equation for $\varphi(k)$ in the form

$$\varphi(k) = \psi_l(\mathbf{k})\Delta_l(\omega), \quad (2.23)$$

where $\psi_l(k)$ is the basis function of the irreducible representation of the point group of the crystal and $\Delta_l(\omega)$ depends only on frequency. Equation (2.20) then leads to the following expression for $T_c$ of the $l$-type superconducting state:

$$T_c = \frac{2\gamma}{\pi}\omega_m \exp\left(-\frac{1 + \lambda}{\lambda_l}\right); \quad (2.24)$$

where $\omega_m$ is the limiting frequency of spin fluctuations and $\lambda_z$ and $\lambda_l$ are the total and partial coupling constants, defined by

$$\lambda_z = \langle\langle V_Z(\mathbf{k}\mathbf{k}'; 0)\rangle\rangle\rho(\mu), \quad (2.25)$$

$$\lambda_l = \langle\langle \psi_l(\mathbf{k})V(\mathbf{k}\mathbf{k}'; 0)\psi_l(\mathbf{k}')\rangle\rangle\rho_l(\mu). \quad (2.26)$$

The double angle brackets represent averaging over the momenta $\mathbf{k}$ and $\mathbf{k}'$ on the Fermi surface; $\rho(\mu)$ is the total density and $\rho_l(\mu)$ the partial density of states on the Fermi surface. The coupling constants are thus averages of the two interactions $V_Z$ and $V$ at zero frequency, as in the usual electron-phonon model of superconductivity.[19] Both $V$ and $V_Z$ are proportional to the magnetic susceptibility $\chi(q)$ which has a peak near the wave vector 0 or $\mathbf{k}_0$ in the case of ferromagnetic or antiferromagnetic susceptibility (Fig. 2).

The coupling constant $\lambda_z$ is positive. The expression for $T_c$ given by (2.24) is meaningful only if $\lambda_l$ is also positive. As already noted, the quantity $V$ that determines $\lambda_l$ is negative, so that $\lambda_l$ can be positive only for a basis function with an alternating sign. For example, for the simple cubic lattice, $\varphi_l(k)$ is given by the following expression in the nearest-

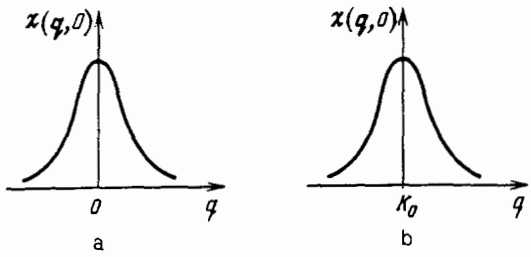


FIG. 2. Magnetic susceptibility near a ferromagnetic (a) and an antiferromagnetic (b) instability.

neighbor approximation for $l$ with s-, p-, and d-wave symmetry[2]

$$\psi_s(\mathbf{k}) = \cos k_x + \cos k_y + \cos k_z,$$
$$\psi_{p1}(\mathbf{k}) = \sin k_x, \quad \psi_{p2}(\mathbf{k}) = \sin k_y, \quad \psi_{p3}(\mathbf{k}) = \sin k_z,$$
$$\psi_{d1}(\mathbf{k}) = \cos k_x - \cos k_y, \quad \psi_{d2}(\mathbf{k}) = 2\cos k_z - \cos k_x - \cos k_y,$$
$$\psi_{d'1}(\mathbf{k}) = \sin k_x \cdot \sin k_y, \quad \psi_{d'2}(\mathbf{k}) = \sin k_x \cdot \sin k_z, \tag{2.27}$$
$$\psi_{d'3}(\mathbf{k}) = \sin k_y \cdot \sin k_z.$$

At half-filling in the simple cubic lattice, nesting occurs for $\mathbf{Q} = (\pi,\pi,\pi)$ (lattice constant $a$ set equal to unity), so that the SDW state with wave vector $\mathbf{k}_0 = \mathbf{Q}$ is produced. At the same time, the basis functions (2.27) have the property

$$\psi_l(\mathbf{k} + \mathbf{Q}) = -\psi_l(\mathbf{k}), \quad l = \mathrm{s}, \mathrm{d}. \tag{2.28}$$

It follows that for states with d-wave symmetry, the expression for $\lambda_l$ given by (2.25) can be rewritten in the form

$$\lambda_l = -\langle\langle \psi_l(\mathbf{k}) V(\mathbf{k} - \mathbf{k}' - \mathbf{Q}; 0) \psi_l(\mathbf{k}') \rangle\rangle \rho_l(\mu), \tag{2.29}$$

where the integration with respect to $\mathbf{k}$ and $\mathbf{k}'$ is carried out over the two Fermi surfaces shifted by the vector $\mathbf{k}_0$. Since the interaction $V(k)$ is proportional to $\chi(k)$, and the latter has a narrow peak near $\mathbf{k} = \mathbf{Q}$ in the case of SDW instability, the quantity $|\mathbf{k} - \mathbf{k}'|$ is small and the integration in (2.29) is performed over a certain region near the line of intersection of the two Fermi surfaces.

Comparing (2.29) with the original (2.26), and recalling the properties of magnetic susceptibility near the boundaries of the magnetic phase transition, we see that the $\lambda_l$ have different signs for ferro- and antiferromagnetic instabilities. The structure of (2.29) suggests that $\lambda_l$ may be negative for the antiferromagnetic instability. Numerical evaluation of $\lambda_l$ has confirmed this.[2] It was found that for fillings corresponding to the boundary of existence of the SDW phase, $\lambda_l$ is positive and much greater when the order parameter has the d-wave symmetry; $\lambda_l$ is negative for s-wave symmetry and negligible for p-wave symmetry (triplet pairing). The numerical magnitude of $\lambda_l$ for d-wave symmetry does not exceed 0.1, so that $T_c$ due to the spin fluctuation mechanism does not exceed a few degrees Kelvin.

### 2.3. Properties of the two-dimensional model

Consider a square lattice with the electron dispersion law

$$\varepsilon_{\mathbf{k}} = -2t(\cos k_x + \cos k_y). \tag{2.30}$$

Figure 3 shows its Brillouin zone in which the thick line represents the isoenergy surface $\varepsilon_{\mathbf{k}} = 0$ corresponding to the half-filled band. In the case of exact half-filling ($n = 1$), we have perfect nesting of the Fermi surface with wave vector $\mathbf{Q} = (\pi,\pi)$.

The density of states has a logarithmic singularity near $\varepsilon = 0$:

$$\rho(\varepsilon) = \frac{1}{2\pi^2 t} \ln \frac{16t}{\varepsilon}, \tag{2.31}$$

so that the magnetic susceptibility $\chi_0(q,\omega)$ has singularities as a function of temperature and chemical potential. For $\mu = 0$ (half-filled band), we then have[20]

$$\chi_0(0,0) \sim \frac{1}{t}\ln\frac{t}{T}, \quad \chi_0(\mathbf{Q},0) \sim \frac{1}{t}\ln^2\frac{t}{T}. \tag{2.32}$$

When $4t \gg \mu \gg t$, we have

$$\chi_0(0,0) \sim \frac{1}{t}\ln\frac{t}{\mu}, \quad \chi_0(\mathbf{Q},0) \sim \frac{1}{t}\ln^2\frac{t}{\mu}. \tag{2.33}$$

Because of these singularities, the equation $1 - U\chi_0(\mathbf{q},0) = 0$ always has a solution either for finite $T$ with $\mu = 0$ or finite $\mu$ with $T = 0$. For a half-filled band, an SDW state is produced in the system with wave vector $\mathbf{k}_0 = \mathbf{Q}$ and magnetic transition point[20]

$$T_m \sim t \exp\left[-2\pi\left(\frac{t}{U}\right)^{1/2}\right]. \tag{2.34}$$

Numerical solution of these equations in the two-dimensional case shows that a superconducting state arises in a certain limited range of hole concentrations near the boundary of the transition to the antiferromagnetic state. Figure 4 shows a typical phase diagram. Superconductivity increases as the boundary of the magnetic phase is approached, but the magnitude of $T_c$ remains exceedingly low. For example, for $U/t = 1.2$, the maximum value is $T_c \approx 2\times 10^{-3}$t. If we choose the parameters so that for $\mu = 0$ (half-filled band), $T_m = 250$ K (for which $4t \approx 6600$ K), then $T_c \lesssim 2.5$ K. As the ratio $U/t$ increases, the region occupied by the superconducting state expands and $T_c$ increases, but does not ex-

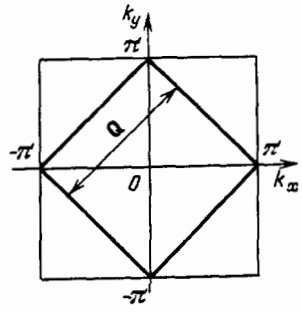


FIG. 3. Brillouin zone for a square lattice.

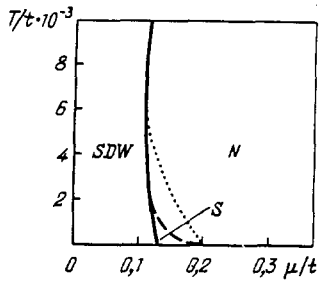


FIG. 4. Phase diagram on the $(T,\mu)$ plane for $U/t = 1$ (Ref. 20). Solid line–magnetic ordering temperature $T_m$, dashed line–superconducting transition point. The dotted line represents $T_c$ without the electron self-energy correction.

ceed a few degrees Kelvin. Superconductivity does not occur at all for $U/t \approx 0.6$. We also note the importance of the self-energy correction to the spectrum, which reduces $T_c$ very considerably despite the fact that the attractive potential for electrons via spin fluctuations diverges for $T = T_m$.

In contrast to the electron-phonon model of superconductivity, in which vertex corrections as measured by the adiabatic parameter $(m/M)^{1/2}$ are small (Ref. 19), in the Hubbard model these corrections are not small *a priori* so that their contribution to $T_c$ may turn out to be significant. The vertex corrections to the electron-spin-fluctuation interactions were first taken into account in Ref. 21 in which their effect on $T_c$ and other parameters of the system were investigated.

Actually, the expression for $\Sigma$ given by (2.16) should include corrections for scattering with spin conservation and with spin flip. However, the analysis given in Ref. 21 includes only the corrections to the vertex part that do not contain transverse spin fluctuations. The correction to the Green's function for paramagnetic states [the quantity $Z(\mathbf{k},i\omega_n)$] is determined in a self-consistent manner. The following simplifications are used in the numerical calculations: the frequency and momentum dependence of $Z$ and $\varphi$ are only partially taken into account, i.e., their dependence on $\omega_n$ is neglected, but the dependence on $\mathbf{k}$ is retained.

A numerical solution of the equations for $Z$ and $\varphi$ shows that corrections to the vertex parts have no effect on the qualitative conclusions about superconductivity in the system due to spin fluctuations: superconductivity is found to persist near the transition to the antiferromagnetic state and the superconducting order parameter has the d-wave symmetry, but the critical temperature $T_c$ is significantly renormalized. Vertex corrections give rise to two opposite processes that affect the magnitude of $T_c$. On the one hand, they produce an increase in the effective mass (through the increase in $Z$) that significantly reduces $T_c$. On the other hand, the vertex corrections lead to an increase in the amplitude for the scattering of electrons by spin fluctuations for scattering vector $\mathbf{Q} = (\pi,\pi)$, which enhances the pairing-interaction kernel in the equation for $\varphi$. The combined effect of these two processes is that $T_c$ increases by several times as compared with the RPA approximation.

## 3. PAIRING OF ELECTRONS VIA SPIN FLUCTUATIONS IN THE ANTIFERROMAGNETIC PHASE

### 3.1. The concept of the spin bag

We have seen that the interaction between electrons via spin fluctuations in the paramagnetic phase near the phase transition to the antiferromagnetic state can lead to superconducting pairing in which the order parameter has the d-wave symmetry. Studies of this pairing mechanism in systems with existing long-range antiferromagnetic order or sufficiently extended short-range magnetic order have assumed considerable importance in connection with the problem of high-temperature superconductivity. If the magnetic correlation length is significantly greater than the correlation length $\xi$ of the superconductor, then the presence or otherwise of long-range magnetic order is unimportant for the evolution of the superconducting state. We can then investigate the effect of electron pairing via spin fluctuations in terms of the two-dimensional Hubbard model in which there is no long-range magnetic order, but the magnetic correlation length can be sufficiently long. It is then convenient to assume that the system behaves as if there was long-range magnetic order.

Effects associated with the influence of antiferomagnetic order on superconducting pairing can be included by taking into account the change in the electron spectrum produced by antiferromagnetic ordering. We know (see, for example, Ref. 4) that magnetic ordering splits the original electron band and the band gap appears precisely at the boundary of the magnetic Brillouin zone. If the Fermi surface lies near such boundaries, the change in the spectrum becomes very significant for all the physical properties of the system. This is precisely the situation in the two-dimensional Hubbard model with a half-filled band ($n = 1$). A gap $\Delta$ then appears on the Fermi surface which coincides with the boundary of the magnetic Brillouin zone, so that the metal becomes an antiferromagnetic insulator.

Schrieffer *et al.*[22] have investigated the behavior of holes in the lower (valence) quasiparticle band by including the effects of their interaction with magnetic fluctuations. Each hole partly destroys the antiferromagnetic order in its immediate neighborhood and becomes localized in this disturbed region, displacing the deformation cloud during its motion. The magnetic polaron produced in this way is referred to by these workers as a 'spin bag'. If there is a second hole with its own spin bag, the overlap between the deformed magnetic structure regions produces an interaction between the holes, and a common bag may be formed with an attendant reduction in total energy. This is the origin of the effective attraction between holes that can lead to Cooper pairing.

In the mathematical implementation of this scheme, we have to solve two series of problems: (1) we have to introduce new quasiparticles that take into account the motion of electrons in the antiferromagnetic lattice and (2) we have to calculate the magnetic susceptibilities of the system and express them in terms of the effective quasiparticle interaction, and then find the effective interaction between the implanted holes in the Cooper channel. The successive stages of this theory are briefly presented below.[22]

We assume that a Néel ground state with wave vector $\mathbf{k}_0$ equal to the nesting vector $\mathbf{Q} = (\pi,\pi)$ is produced in our

square lattice at half-filling. Spontaneous symmetry breaking leads to a change in the electron spectrum that is readily determined in the mean-field approximation. We now replace the Hamiltonian (1.1) with the quadratic form

$$\mathcal{H}_{\mathrm{MF}} = \sum_{\mathbf{k}} \varepsilon_{\mathbf{k}} (c^{+}_{\mathbf{k}\uparrow} c_{\mathbf{k}\uparrow} + c^{+}_{\mathbf{k}\downarrow} c_{\mathbf{k}\downarrow}) - \Delta \sum_{\mathbf{k}} (c^{+}_{\mathbf{k}+\mathbf{Q}\uparrow} c_{\mathbf{k}\uparrow} - c^{+}_{\mathbf{k}+\mathbf{Q}\downarrow} c_{\mathbf{k}\downarrow}) \tag{3.1}$$

in which the parameter $\Delta$ is found from the self-consistency condition.

The diagonalization of $\mathcal{H}_{\mathrm{MF}}$ is achieved by the canonical transformation to new Fermi operators that mix the electron states with momenta $\mathbf{k}$ and $\mathbf{k}+\mathbf{Q}$:

$$\gamma^{c}_{\mathbf{k}\alpha} = u_{\mathbf{k}} c_{\mathbf{k}\alpha} - v_{\mathbf{k}} \sum_{\beta} \sigma^{z}_{\alpha\beta} c_{\mathbf{k}+\mathbf{Q}\beta},$$
$$\gamma^{v}_{\mathbf{k}\alpha} = v_{\mathbf{k}} c_{\mathbf{k}\alpha} + v_{\mathbf{k}} \sum_{\beta} \sigma^{z}_{\alpha\beta} c_{\mathbf{k}+\mathbf{Q}\beta}, \tag{3.2}$$

where the real coefficients $u_{\mathbf{k}}$ and $v_{\mathbf{k}}$ satisfy the condition $u^2_{\mathbf{k}} + v^2_{\mathbf{k}} = 1$, $\alpha$ and $\beta$ are the spin indices, and $\sigma^z$ is the Pauli matrix ($z$ is the direction of the spontaneous magnetic moment of the sublattices). In terms of the new operators,

$$\mathcal{H}_{\mathrm{MF}} = \sum_{\mathbf{k},\alpha}{}' E_{\mathbf{k}} (\gamma^{+c}_{\mathbf{k}\alpha} \gamma^{c}_{\mathbf{k}\alpha} - \gamma^{+v}_{\mathbf{k}\alpha} \gamma^{v}_{\mathbf{k}\alpha}), \tag{3.3}$$

where

$$E_{\mathbf{k}} = (\varepsilon^2_{\mathbf{k}} + \Delta^2)^{1/2}. \tag{3.4}$$

In one of the two bands, namely, the conduction band (with the operator $\gamma^c$), the quasiparticle energy is $E_{\mathbf{k}}$ whereas in the other band, namely, the valence band (with the operator $\gamma^v$), the quasiparticle energy is $-E_{\mathbf{k}}$ (Fig. 5). The prime on the sum over $\mathbf{k}$ represents summation over the magnetic Brillouin zone lying inside the region

$$-\pi < k_x < \pi, \quad -\pi + k_x < k_y < \pi - k_x, \tag{3.5}$$

that occupies an area smaller by a factor of two than the original Brillouin zone (see Fig. 3).

For a half-filled original band ($n = 1$), the valence band is completely filled whereas the conduction band is empty, so that the system is an insulator with a gap $2\Delta$. It is clear from (3.4) that $\Delta$ is the gap in the spectrum of the single-particle excited state that is either a hole in the valence band or a particle in the conduction band. The size of the gap is found from the self-consistency equation

$$\frac{1}{N} \sum_{\mathbf{k}}{}' \frac{1}{(\varepsilon^2_{\mathbf{k}} + \Delta^2)^{1/2}} = \frac{1}{U}. \tag{3.6}$$

Collective excitations of the system are determined by the poles of the magnetic susceptibility $\chi$. In the RPA approximation, $\chi$ is found by summing over the same loop diagrams that arose in the evaluation of the susceptibility in the paramagnetic phase [see (2.5)]. For the magnetically ordered state, there are two differences: first, the Green line loops correspond not to electrons but to quasiparticles with energies $E_{\mathbf{k}}$ and $-E_{\mathbf{k}}$ and, second, the loss of translational invariance means that $\chi$ should depend on the two momenta $\mathbf{q}$ and $\mathbf{q}'$.

The self-energy correction must be calculated for the electron in order to take into account fluctuation effects in the sublattice magnetization. We shall take it in the following form (for example, for an electron with spin $\uparrow$)

$\Sigma_{\uparrow} =$ 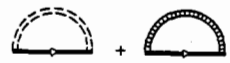 ; (3.7)

where the double dashed line represents the effective interaction via the electron loops whereas the double shaded line represents the sum of all the antiparallel ladder diagrams. The first graph is thus seen to describe processes with the conservation of spin whereas the second describes processes with spin flip due to the interaction with longitudinal and transverse (spin wave) fluctuations above the SDW state. The effective interaction lines have analytic expressions for $V^z$ and $V^{+-}$. They, and also the susceptibilities $\chi^{zz}$ and $\chi^{+-}$, are functions of the two momenta $\mathbf{q}$ and $\mathbf{q}'$, but $\chi^{zz}$ is diagonal whereas $V^{+-}$ contains an off-diagonal contribution due to the term $\chi^{+-}_{Q}$ which is an odd function of $\omega$ and is therefore small for small $\omega \leqslant \Delta$. If we neglect this contribution, we obtain the following expressions for the longitudinal and transverse effective interactions:

$$V^{z}(\mathbf{q}, \omega) = \frac{U^2 \chi^{zz}_0(\mathbf{q}, \omega)}{1 - U\chi^{zz}_0(\mathbf{q}, \omega)}, \tag{3.8}$$

$$V^{+-}(\mathbf{q}, \omega) = \frac{U^2 \chi^{+-}_0(\mathbf{q}, \omega)}{1 - U\chi^{+-}_0(\mathbf{q}, \omega)}; \tag{3.9}$$

where

$$\chi_0(\mathbf{q}, \omega) = -\frac{1}{2N} \sum_{\mathbf{k}}{}' \left(1 - \frac{\varepsilon_{\mathbf{k}}\varepsilon_{\mathbf{k}+\mathbf{q}} \pm \Delta^2}{E_{\mathbf{k}} E_{\mathbf{k}+\mathbf{q}}}\right) \times \left(\frac{1}{\omega - E_{\mathbf{k}+\mathbf{q}} - E_{\mathbf{k}} + i\delta} + \frac{1}{-\omega - E_{\mathbf{k}+\mathbf{q}} - E_{\mathbf{k}} + i\delta}\right), \tag{3.10}$$

in which the upper sign in front of $\Delta^2$ is taken for the component $\chi^{zz}_0$ and the lower for $\chi^{+-}_0$.

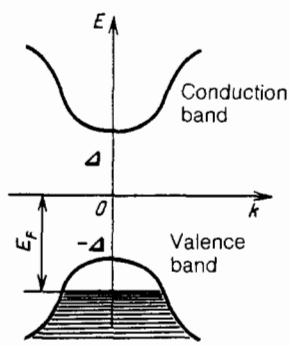


FIG. 5. Quasiparticle energy spectrum in the SDW state.

We now turn to the interaction between two holes in a half-filled band. In the static approximation, this interaction is described by (3.8) and (3.9) with $\omega = 0$. The effective interaction Hamiltonian for holes in the longitudinal and transverse channels is determined in accordance with the expressions[23]

$$H_z = -\frac{1}{4N}\sum_{\mathbf{k},\mathbf{k}',\mathbf{q}}\sum_{\alpha,\alpha',\beta,\beta'} V^z(\mathbf{k}-\mathbf{k}',0)\sigma^z_{\alpha'\alpha}\sigma^z_{\beta'\beta} \times c^+_{\mathbf{k}'\alpha'}c^+_{-\mathbf{k}'+\mathbf{q}\beta'}c_{-\mathbf{k}+\mathbf{q}\beta}c_{\mathbf{k}\alpha}, \tag{3.11}$$

$$H_{+-} = -\frac{1}{4N}\sum_{\mathbf{k},\mathbf{k}',\mathbf{q}}\sum_{\alpha,\alpha',\beta,\beta'} V^{+-}(\mathbf{k}-\mathbf{k}',0)\sigma^+_{\alpha'\alpha}\sigma^-_{\beta'\beta} \times c^+_{\mathbf{k}'\alpha'}c^+_{-\mathbf{k}'+\mathbf{q}\beta'}c_{-\mathbf{k}+\mathbf{q}\beta}c_{\mathbf{k}\alpha}, \tag{3.12}$$

where $\sigma^{+-} = \sigma^x \pm i\sigma^y$. We now perform the reverse transformation in (3.2), from the electron operators to the quasiparticle operators. The Hamiltonian written in the terms of the operators $\gamma^v$ and $\gamma^c$ contains different contributions, including interband transitions. Since, the valence and conduction bands are separated by the large gap $2\Delta$, interband transitions can be neglected. We then obtain the following expressions for the hole Hamiltonians describing interactions via longitudinal and transverse fluctuations in the Cooper channel (total momentum of a pair $q = 0$)[23]

$$H_z = -\frac{1}{4N}\sum'_{\mathbf{k},\mathbf{k}'}\sum_{\alpha,\alpha',\beta,\beta'}\Big(V^z(\mathbf{k}-\mathbf{k}',0)l^2(\mathbf{k}\mathbf{k}')\sigma^z_{\alpha'\alpha}\sigma^z_{\beta'\beta} + V^z(\mathbf{k}-\mathbf{k}'+\mathbf{Q},0)m^2(\mathbf{k}\mathbf{k}')\delta_{\alpha'\alpha}\delta_{\beta'\beta}\Big)\gamma^{+v}_{\mathbf{k}'\alpha'}\gamma^{+v}_{-\mathbf{k}'\beta'}\gamma^v_{-\mathbf{k}\beta}\gamma^v_{\mathbf{k}\alpha}, \tag{3.13}$$

$$H_{+-} = -\frac{1}{4N}\sum'_{\mathbf{k},\mathbf{k}'}\sum_{\alpha,\alpha',\beta,\beta'}\Big(V^{+-}(\mathbf{k}-\mathbf{k}',0)n^2(\mathbf{k}\mathbf{k}') - V^{+-}(\mathbf{k}-\mathbf{k}'+\mathbf{Q},0)\Big)\sigma^+_{\alpha'\alpha}\sigma^-_{\beta'\beta}\gamma^{+v}_{\mathbf{k}'\alpha'}\gamma^{+v}_{-\mathbf{k}'\beta'}\gamma^v_{-\mathbf{k}\beta}\gamma^v_{\mathbf{k}\alpha}, \tag{3.14}$$

where we have introduced the so-called coherence factors

$$m(\mathbf{k}\mathbf{k}') = u_{\mathbf{k}}v_{\mathbf{k}'} + v_{\mathbf{k}}u_{\mathbf{k}'}, \quad p(\mathbf{k}\mathbf{k}') = u_{\mathbf{k}}v_{\mathbf{k}'} - v_{\mathbf{k}}u_{\mathbf{k}'},$$
$$l(\mathbf{k}\mathbf{k}') = u_{\mathbf{k}}u_{\mathbf{k}'} + v_{\mathbf{k}}v_{\mathbf{k}'}, \quad n(\mathbf{k}\mathbf{k}') = u_{\mathbf{k}}u_{\mathbf{k}'} - v_{\mathbf{k}}v_{\mathbf{k}'}. \tag{3.15}$$

The expressions in parentheses in (3.13) and (3.14) represent the effective interactions of quasiparticles in the valence band via longitudinal and transverse spin fluctuations. In addition to the two interaction channels $H_z$ and $H_{+-}$ between holes via spin fluctuations, there is also the channel $H_c$ in which the interaction takes place via charge fluctuations. This channel is omitted here because the energies of the corresponding collective modes lie much higher than the energies of the spin modes, so that this particular channel is ineffective in the pairing interaction between the holes.[22]

When the hole concentration is very low, the Fermi surface obviously lies near the magnetic Brillouin zone where $\varepsilon_k = 0$, so that $u_{\mathbf{k}} \approx v_{\mathbf{k}} \approx 1/\sqrt{2}$. The consequence of this is that $p^2(\mathbf{k}\mathbf{k}') \approx n^2(\mathbf{k}\mathbf{k}') \approx 0$. This does not mean, however, that the matrix element of the effective interaction via the spin waves is small, as was initially assumed in Ref. 22. This is not the case because $V^{+-}$ has a singularity. Let us therefore separately examine the effects of each of the terms $H_z$ and $H_{+-}$ in the pairing interaction between holes.

### 3.2. Allowance for longitudinal magnetization fluctuations

We begin with the interaction due to longitudinal fluctuations.[22] The expression given by (3.13) contains only the static interaction. To take the dynamic character of the interaction into account we have to investigate its frequency dependence. The function $V^z(\mathbf{q},\omega)$ is proportional to the longitudinal magnetic susceptibility $\chi^{zz}(\mathbf{q},\omega)$. It does not diverge in the SDW state for momentum $\mathbf{q} = \mathbf{Q}$ as is the case in the paramagnetic phase, but numerical calculations[22] show that, for this wave vector, $\chi^{zz}(\mathbf{q},\omega)$ is largely confined to frequencies not exceeding $2\Delta$, so that we have to introduce the corresponding cutoff frequency $\omega_a \approx 2\Delta$. This cutoff corresponds to a momentum cutoff, so that the matrix element for the singlet channel in (3.13) must be taken to be

$$V_{\mathbf{k}\mathbf{k}'} = \Big(-m^2(\mathbf{k}\mathbf{k}')U^2\chi^{zz}(\mathbf{k}-\mathbf{k}'+\mathbf{Q},0) + l^2(\mathbf{k}\mathbf{k}')U^2\chi^{zz}(\mathbf{k}-\mathbf{k}',0)\Big) \times\theta(\omega_a - |E_{\mathbf{k}} - E_F|)\theta(\omega_a - |E_{\mathbf{k}'} - E_F|), \tag{3.16}$$

where $\theta(x)$ is equal to 1 for $x > 0$ and 0 for $x < 0$. Since $\mathbf{k} - \mathbf{k}'$ is bounded by a small Fermi surface (in the case of a low hole concentration), the second term in (3.16) can be neglected, and it is then clear that $V_{\mathbf{k}\mathbf{k}'}$ is negative, which corresponds to attraction.

Attraction between the holes gives rise to a superconducting gap that can be found from the BCS theory and is given by

$$\Delta_{\mathbf{k}} = -\sum'_{\mathbf{k}'} V_{\mathbf{k}\mathbf{k}'}\frac{\Delta_{\mathbf{k}'}}{\left[(E_{\mathbf{k}'} - E_F)^2 + \Delta^2_{\mathbf{k}'}\right]^{1/2}}. \tag{3.17}$$

Since the pairing interaction $V_{\mathbf{k}\mathbf{k}'}$ is anisotropic, the solution of this equation for $\Delta_{\mathbf{k}}$ is also anisotropic. To determine the symmetry of the solution, i.e., the superconducting order parameter, we have to take into account all the symmetry properties of the pairing interaction. It is found to be antiperiodic in reciprocal space:

$$V_{\mathbf{k}\mathbf{k}'} = -V_{\mathbf{k},\mathbf{k}'+\mathbf{Q}} = -V_{\mathbf{k}+\mathbf{Q},\mathbf{k}'}, \tag{3.18}$$

which follows from the properties of the coefficients of the $u - v$ transformation: $u_{\mathbf{k}+\mathbf{Q}} = v_{\mathbf{k}}$, $v_{\mathbf{k}+\mathbf{Q}} = u_{\mathbf{k}}$. This leads to the antiperiodicity of the order parameter itself:

$$\Delta_{\mathbf{k}} = -\Delta_{\mathbf{k}+\mathbf{Q}}. \tag{3.19}$$

This condition shows that $\Delta_{\mathbf{k}}$ should have zeros in the magnetic Brillouin zone. However, it does not signify that the gap $\Delta_{\mathbf{k}}$ on the Fermi surface must necessarily vanish. Everything depends on the type of the Fermi surface. When the hole concentration is low, the minimum quasiparticle-hole energy should lie at a symmetric point on the boundary of the magnetic Brillouin zone, so that the most probable variants of the Fermi surface are as shown in Fig. 6. The difference between them is that, in case a, all four parts of the

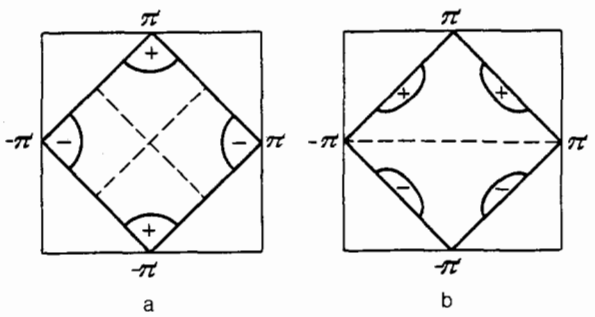


FIG. 6. Two variants of the hole Fermi surface: a–singly connected, b–doubly connected, leading to d-wave and p-wave symmetry of the superconducting order parameter.[22]

Fermi surface can be made coincident on a single closed surface by shifting them by the reciprocal magnetic lattice vector **Q**. This closed surface can then be placed at the center of the magnetic band by a change of its origin. A superposition of pairs is possible in case b, so that the Fermi surface consists of two unconnected surfaces.

The signs + and − indicate the antiperiodicity (3.19) of the superconducting order parameter. In case a, only low momenta **k** and **k**′ participate in the solution, so that the pairing potential $V_{\mathbf{kk}'}$ can be approximated by a constant. Since this is negative, equation (3.17) yields a solution that is homogeneous in the neighborhood of the Fermi surface. Well away from it, $\Delta_{\mathbf{k}}$ can vanish on the dashed lines, but these are the lines representing the boundary of the magnetic Brillouin zone (after the origin has been shifted from the center to a corner). However, a large gap due to the SDW state is present on this line. It follows that $\Delta_{\mathbf{k}}$ does not vanish at any point on the Fermi surface, so that we do not expect in this model to have superconducting variables that are functions of powers of the temperature. A similar conclusion can be drawn for the other variant of the Fermi surface (see Fig. 6b). In the latter case, we must remember that the superconducting order parameter may be degenerate. In addition to the state shown in Fig. 6b, there is another possible state that can be obtained from it by rotation through 90°. Analysis shows that a p-symmetric superconducting parameter appears in the case of a singly connected Fermi surface, and a d-symmetric parameter is obtained in the case of a doubly connected surface.[22]

It is a striking fact that, in this case, the order parameter has no zeros on the Fermi surface although the d- and p-symmetric functions must vanish at certain points in the Brillouin zone. In view of the foregoing, the superconducting order parameter obtained in this model has many of the usual properties typical for s-wave symmetry.

We also note that the order parameter $\langle \gamma^{v}_{\mathbf{k}\uparrow} \gamma^{v}_{\mathbf{k}\downarrow} \rangle$ corresponds to a mixed state that includes a singlet and the $z$-component of the triplet. This occurs because the pair wave function cannot be written as a product of functions of the coordinates alone and of the spin alone, since the orbital functions for spin ↑ and spin ↓ are different (electrons with opposite spins in the SDW state belong to different sublattices).

The d-wave superconducting parameter is obtained independently in a number of papers.[24–27] The possibility of p-wave symmetry is demonstrated in Ref. 28.

Similar questions are discussed in Ref. 29 and in other publications by this author. The results reported in these papers are reviewed critically in Ref. 22. The change in sign of the superconducting order parameter in different energy ranges or different regions of **k**-space is discussed in Refs. 30 and 31.

### 3.3. Allowance for transverse spin fluctuations

We now recall that our calculations included only part of the effective interaction between the holes, namely, the interaction via spin fluctuations. Spin bag theory is based on this idea.[22] We must now take into account the other part of the interaction of holes $H_{+-}$ via spin waves.

The spin-wave spectrum is determined by the poles of the transverse magnetic susceptibility. The poles of the initial susceptibility (3.10) give a continuum of two-particle excitations (hole in the valence band and particle in the conduction band), and it is clear from (3.10) that this spectrum begins for frequencies $\omega > 2\Delta$. The collective branch of the spectrum (the spin wave) lies precisely in this gap[32] (Fig. 7). In the limit in which $U \gg t$, the spin-wave spectrum coincides with the spectrum obtained in the Heisenburg model.[33]

Let us now consider the matrix element of the hole interaction $H_{+-}$ via the spin waves. When the hole concentration is low, $u_{\mathbf{k}} \approx v_{\mathbf{k}} \approx 1/\sqrt{2}$ so that the coherence factors $p(\mathbf{kk}')$ and $n(\mathbf{kk}')$ tend to zero, but, as noted in Ref. 23, the matrix element $V^{+-}$ has a singularity that compensates the low values of the coherence factors. Suppose that the hole Fermi surface lies near the point $(\pi/2,\pi/2)$ and its equivalent $(-\pi/2,-\pi/2)$. For small deviations from it, $\delta k_x = k_x - \pi/2$ and $\delta k_y = k_y - \pi/2$ we have

$$p^2(\mathbf{kk}') \approx \frac{t^2}{\Delta^2}(q_x + q_y)^2, \quad V_{+-}(\mathbf{q} + \mathbf{Q}, 0) \sim \frac{1}{t^2 q^2}, \tag{3.20}$$

where $\mathbf{q} = \mathbf{k} - \mathbf{k}'$ is a vector that is small in comparison with the reciprocal lattice vector. For intermediate values of the parameter $U/t$, the two interactions are comparable in magnitude, but the interaction via the spin waves begins to predominate as $U/t$ increases.

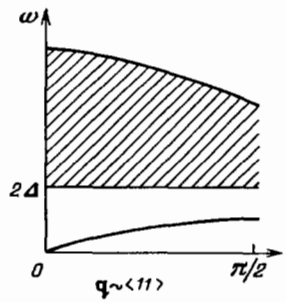


FIG. 7. Spectrum of two-particle excitations and spin waves for the SDW state for $U/t = 4$ (Ref. 32).

Analysis of the pairing potentials $H_z(r)$ and $H_{+-}(r)$ corresponding to (3.13) and (3.14) in real space, shows that the longitudinal part of the potential predominates for small $U/t$ and leads to a singlet Cooper pairing inside the Néel antiferromagnetic ordering. An increase in $U/t$ is accompanied by a rise in the transverse part of the potential, which leads to a helical distortion of the Néel structure in which the rotation of the spins occurs in the $(x,y)$ plane. The pairing potential is weakened and thereafter the increase in $U/t$ should be accompanied by the establishment of the normal helical phase.

Since there is no long-range magnetic order in the two-dimensional Hubbard model at finite temperature, the above theory, which presupposes the existence of long-range magnetic order, must be understood as referring to the limit $l_m \gg \xi_m$, where $l_m$ is the correlation length for the SDW state and

$$\xi_m = \hbar v_F/\Delta \tag{3.21}$$

is the coherence length, i.e., the size of the region around the particle hole in which long-range magnetic order is destroyed and which moves together with the particle.

When the above inequality between the two lengths $l_m$ and $\xi_m$ is not satisfied, we have to approach the problem from the side of the paramagnetic phase and take account of the structure of magnetic susceptibility, which reflects the fluctuations in magnetic order in the system in greater detail. The essential point is that we have to take into account the rapid increase in $\chi(\mathbf{q},\omega)$ at momentum $\mathbf{q} = \mathbf{Q}$. If we then calculate the correction to $\Sigma$ in the form of a graph from (3.7), we can evaluate the density of states near the Fermi surface. It has been found[34] that there are two peaks for free electrons above and below the Fermi level, which correspond to two types of quasiparticle, but between them there is a finite density of states that increases with increasing $U/t$. This means that instead of a gap on the Fermi surface, revealed in the state with long-range SDW order, we now have a pseudogap. For a fixed $U$, the pseudogap depends on the chemical potential and its depth increases as the hole concentration tends to zero. An increase in $U$ is thus seen to produce a crossover from the usual Fermi liquid behavior of the system [with one peak in $\rho(\omega)$ near the Fermi level] to $\rho(\omega)$ with a gap in the SDW state via an intermediate state with the pseudogap.

As in the case of the SDW state, the pairing potential $V_{\mathbf{kk}'}$ between two spin bags in the case of short correlation lengths $l_m$ is attractive for the transition momentum $\mathbf{q} = \mathbf{k} - \mathbf{k}'$, which is less than $\xi_m^{-1}$, due to the fact that two holes prefer to produce a common bag and reduce the energy thereby. However, for large $\mathbf{q} \approx \mathbf{Q}$, the potential $V_{\mathbf{kk}'}$ is repulsive as in the case of the SDW state because spin-fluctuation exchange is known to lead to repulsion in the singlet channel. This means that, if the Fermi surface consists of four pockets at $(\pm\pi/2, \pm\pi/2)$ in the magnetic Brillouin zone, then the superconducting gap in each of them will be nonzero, but its sign will alternate as we pass from one pocket to the next because this is accompanied by a change in momentum by the vector $\mathbf{Q}$. Thus, as in the case of the SDW state, the superconducting gap does not vanish anywhere on the Fermi surface but the superconducting order parameter has overall p-wave symmetry. In the other case, when we have a single-sheet Fermi surface, we are entitled to expect a more usual behavior for the d-wave superconducting gap.

Only qualitative conclusions were drawn in Ref. 34 about the nature of the pairing potential, but the theory is not good enough at present to enable us to estimate the superconducting transition temperature. It must also be remembered that the cutoff frequencies in the longitudinal and transverse parts of the interaction should be different in the SDW phase because of the difference between the nature of spin fluctuations in this phase. In the case of the $H_{+-}$ term, we have spin waves, i.e., satisfactorily propagating excitations, whereas for the $H_z$ term we have nondispersive diffusion modes.

Superconducting pairing via spin fluctuations is thus more likely for small values of $U/t$ for which the contribution of longitudinal fluctuations is predominant. An increase in $U/t$ is at first accompanied by predominant repulsion in the singlet channel via the interaction with the spin waves, which has long been established within the framework of the s – d exchange model of a metal.[4] The possible existence of the superconducting state is therefore determined by a balance between two opposing contributions. Finally, further increase in $U/t$ should give rise to helical magnetic ordering as noted above. However, here we enter the strong coupling regime for which RPA ceases to be valid. In this situation, we have to start with the opposite limit, i.e., $U/t \gg 1$, which is equivalent to using the $t-J$ model. It is within the framework of this model that the existence of the helical phase was first established.[35,36] We shall return to this question in the second part of this review.

There are several publications[37–44] that discuss the approach from the side of $U \ll W$ and report more accurate determinations of magnetic states in the two-dimensional Hubbard model near half-filling. A fundamental analysis of the ground state is reported in Ref. 37 in which it is shown that the antiferromagnetic Néel state with long-range order is unstable against the formation of an antiferromagnetic state with short-range order and helical magnetic structure when the hole concentration is low. Hole density fluctuations generate fluctuations in helical order, and the correlation between these magnetic fluctuations behaves exponentially over distances of the order of the mean hole separation. A similar behavior of magnetic fluctuations has been observed in high-$T_c$ materials (see the review in Ref. 15). The hole Fermi surface is formed around the points $(\pm\pi/2, \pm\pi/2)$, which leads to $p$-wave symmetry of the superconducting order parameter.

The helical structure is not the only type of instability of the Néel state that is found to be present when holes are introduced. Variational methods and the Hartree–Fock approximation are used in Refs. 40–42 to show that the antiferromagnetic domain structure with periodically distributed domain walls (soliton lattice) has a lower energy that the Néel state. A variational Monte Carlo method is used in Ref. 40 to show that this occurs for $U = 4t - 10t$. The hole distribution should not be homogeneous in this structure. In fact, it is found that holes tend to congregate near domain walls, which gives rise to one-dimensional polarization of the medium. It is also found that the incommensurate antiferromagnetic phase is unstable with respect to superconductivity.

Moreover, the fundamental study reported in Ref. 43

shows that the magnetic structure of the ground state may turn out to be much more complicated than any incommensurate phase in the two-dimensional Hubbard model near $n = 1$. It is found that the solution of the Hartree–Fock equations leads to a dense set of localized states that includes magnetic polarons, domain walls, and vortices with very similar energies. The authors of Ref. 43 maintain that the large number of almost degenerate solutions of the Hartree–Fock equations is a specific property of the two-dimensional Hubbard model near half-filling. These solutions correspond to metastable states. For intermediate values $U \sim W$, the system can be described as a liquid with a strong interaction between nonlinear structure elements. The most likely conclusion is that, in this regime, the liquid is unstable against Cooper pairing. For high $U \gg W$, the system is best described in terms of vortices with a small core and low mobility due to transverse spin fluctuations. If allowance for fluctuations beyond the limit of the Hartree–Fock approximation does not remove the above degeneracy of metastable spin and charge fluctuations, the system may be found exceptionally difficult for analytic and even numerical investigation, which is analogous to the situation in the case of spin glasses.

Thus, as we go into the theory of the two-dimensional Hubbard model near half-filling, it becomes evident that the ground-state problem is very complicated even for low and moderate values of the Coulomb repulsion $U \lesssim W$. This applies not only to the superconducting state problem, but also to the magnetic structure. Different answers are obtained for the structure of the magnetic state of the system, depending on which approximation is employed. In this situation, numerical methods that do not use what is essentially a perturbation theory in the parameter $U/W$ assume particular importance.

## 4. MOTION OF A HOLE IN A TWO-DIMENSIONAL ANTIFERROMAGNET WITH HALF-FILLING

### 4.1. Perturbation theory results

Although we have already investigated (in the last Section) the interaction between holes in the SDW state of the system for the half-filled initial band, we must now turn to the single-hole problem and examine in greater detail the properties of the single-particle state such as damping, effective mass, and coherent state intensity. The last of these is particularly important in connection with the Fermi-liquid picture of implanted holes, i.e., essentially the Fermi surface. This was implicitly assumed in our discussion of hole interaction effects.

There are two approaches to this problem: one is based on perturbation theory in the parameter $U/t$ from which the results are usually extended to the region $U \sim t$ without any particular justification; the other approach uses numerical simulation in which one considers the intermediate region $U \sim t$. We shall examine these two approaches in the present Section, leaving the strong coupling regime $U/t \gg 1$ to the second part of our review. We begin with perturbation theory.

We must explicitly investigate the corrections to the self-energy of electrons that are due to the interaction with spin fluctuations in the SDW state. Magnetic order in the system at half-filling was taken into account in the mean-field approximation, and the electron Green's function depends on two momenta because of the change in the translational symmetry introduced by antiferromagnetic order. It takes the form of a $2\times2$ matrix:[32]

$$G^{0\sigma}(\mathbf{k},\omega) = \begin{pmatrix} \omega+\varepsilon_{\mathbf{k}} & \sigma\Delta \\ \sigma\Delta & \omega-\varepsilon_{\mathbf{k}} \end{pmatrix} \frac{1}{\omega^2 - E_{\mathbf{k}}^2 + i\delta}. \tag{4.1}$$

The first row of the matrix corresponds exactly to the expression for $G^0_{\alpha\beta}(\mathbf{k}\mathbf{k}';\omega)$ whereas the second row corresponds to the expression for $G^0_{\alpha\beta}(\mathbf{k}+\mathbf{Q},\mathbf{k}';\omega)$ that takes into account the fact that $\varepsilon_{\mathbf{k}+\mathbf{Q}} = \varepsilon_{\mathbf{k}}$. The fact that the result is diagonal in the spin indices $\alpha, \beta$ has also been taken into account. Although this function is defined for real electrons, it also describes the motion of quasiparticles with energy $E_{\mathbf{k}}$ in the conduction band and energy $-E_{\mathbf{k}}$ in the valence band. Figure 5 shows the structure of the spectrum in this approximation.

The interaction between electrons and spin fluctuations leads in the RPA to the self-energy correction $\Sigma^{\sigma}(\mathbf{k},\omega)$ represented by the graphs of (3.7). The improved Green's function $G^{\sigma}(\mathbf{k},\omega)$ will now be found from the Dyson equation

$$G^{\sigma^{-1}}(\mathbf{k},\omega) = G^{0\sigma^{-1}}(\mathbf{k},\omega) - \Sigma^{\sigma}(\mathbf{k},\omega), \tag{4.2}$$

where each term is a $2\times2$ matrix in reciprocal space. It is readily verified that, if we write down the analytic expression for $\Sigma^{\sigma}(\mathbf{k},\omega)$, we find that it does not depend on the spin projection $\sigma$. The spectrum $\varepsilon_{\mathbf{k}}$, the damping constant $\Gamma_{\mathbf{k}}$, and the intensity $a_{\mathbf{k}}$ of the single-particle peak are described in the following way in terms of $\Sigma_+ = \Sigma_{11} + \Sigma_{12}$ where $\Sigma_{\alpha\beta}$ is the matrix element of the self-energy part:

$$\omega = \Delta + \Sigma_+(\mathbf{k},\omega), \tag{4.3}$$

$$\Gamma_{\mathbf{k}} = -\operatorname{Im}\Sigma_+(\mathbf{k},\omega)\cdot\left(1 - \frac{\partial \operatorname{Re}\Sigma_+(\mathbf{k},\omega)}{\partial\omega}\bigg|_{\omega=\varepsilon_{\mathbf{k}}}\right)^{-1}, \tag{4.4}$$

$$a_{\mathbf{k}} \equiv \frac{1}{Z_{\mathbf{k}}} = \left(1 - \frac{\partial \operatorname{Re}\Sigma_+(\mathbf{k},\omega)}{\partial\omega}\bigg|_{\omega=\varepsilon_{\mathbf{k}}}\right)^{-1}. \tag{4.5}$$

Numerical calculations of these quantities for a number of points in the magnetic Brillouin zone demonstrate the existence of well-defined quasiparticles. The intensity of the quasiparticle peak falls substantially with increasing $U/t$ because of the contribution of incoherent states that are not taken into account in this analysis. For $U/t = 10$ we already have $Z_{\mathbf{k}} = 4.5$ [the energy at $(\pi/2,\pi/2)$ is $\varepsilon_{\mathbf{k}} = 0.897t$] whereas for $U/t = 80$ we have $Z_{\mathbf{k}} = 200$ [$\varepsilon_{\mathbf{k}} = 8.487t$ at $(\pi/2,\pi/2)$]. As far as the damping constant is concerned, this is also small in both these cases and its order of magnitude is $\Gamma_{\mathbf{k}} \sim 10^{-3}t$.

We therefore conclude that satisfactory quasiparticle properties of the holes persist in a wide range of values of $U/t$ for low hole concentrations.

The other important conclusion from these data is that the energy minimum lies at $(\pi/2,\pi/2)$. This means that when the system is doped, the hole Fermi surface is formed around the points $(\pm\pi/2, \pm\pi/2)$. Calculations show that a closed Fermi surface that is highly elongated along the band boundary evolves around the point $(\pi/2,\pi/2)$. Similar

surfaces appear around other equivalent points. Hence, the Fermi surface has a multivalley topology for low hole concentrations. A singly-connected surface with the center at (0,0) appears at a certain energy ($\varepsilon_k = 0.248t$). This limiting surface encompasses roughly 85% of the area of the Brillouin zone, from which it follows that the topology of the Fermi surface should undergo a change for hole concentration $n_h = 0.15$.

The conclusion that the quasihole energy minimum lies at $(\pi/2,\pi/2)$ was deduced in Ref. 32 by numerical methods and was then confirmed by analytic calculations in the limit as $U \to \infty$. However, this conclusion is in conflict with the predictions reported in an earlier paper,[44] which indicate that the minimum should be at $(\pi,0)$. We recall that a minimum at $(\pi/2,\pi/2)$ gives rise to the p-wave symmetry of the solution of the BCS equation for the superconducting gap. It is therefore clear that the hole Fermi surface in this model and, hence, the symmetry of the superconducting order parameter, require further elucidation.

### 4.2. Numerical calculations by the quantum Monte-Carlo method

In the intermediate regime $U \sim t$ and for high values of the Coulomb repulsion parameter, direct numerical methods provide more reliable information. The two-dimensional Hubbard model was recently investigated in detail, using a specially developed quantum Monte-Carlo method (QMCM).[45,46] One of the general limitations of this method in relation to Fermi systems is that the temperature must be sufficiently high. The authors of Ref. 45 and 46 succeeded in developing algorithms that can be used only for cluster systems of the order of 10–100 sites on a lattice.

Comparison of calculations made for clusters of different size ($6\times6, 16\times16$) demonstrates the stability of the physical results for such cluster dimensions. The calculations were performed for electron concentrations $n = 1$ and 0.5 and also for certain intermediate values at $T = t/6$ and different values of $U/t$. Among the characteristics of electron states that were investigated were the particle momentum distribution, energy gap, damping constant, and magnetic structure. The last of these can be described by the magnetic structure factor

$$S(\mathbf{q}) = \frac{1}{N}\sum_i e^{i\mathbf{q}\mathbf{R}_i}\langle m_{i+l}^z m_i^z\rangle, \tag{4.6}$$

where $m_i^z = n_{i\uparrow} - n_{i\downarrow}$ is the spin density on the lattice. The results can be summarized as follows.

At half-filling ($n = 1$), the function $S(\mathbf{q})$ calculated for an $8\times8$ cluster has a well-defined peak for $\mathbf{Q} = (\pi,\pi)$ (Fig. 8), which suggests an implicit magnetic short-range order at a finite temperature. As the filling is reduced ($n = 0.83$), the peak shifts along the line $(\pi,\pi - \Delta q)$, where $\Delta q = 0.3$, or in the equivalent direction $(\pi - \Delta q,\pi)$. The height of the peak becomes several times lower. For $n = 0.72$, the peak is lower still and broader, and is found to be shifted in the same direction by the amount $\Delta q = 0.4$. The structure factor peak is thus seen to shift not along the diagonal of the reciprocal lattice cell, but along its edge. This agrees with the RPA predictions and numerical calculations performed in Ref. 47 by a different method. Of course, it would be desirable to know whether this peak diverges for $n < 1$ as the cluster size

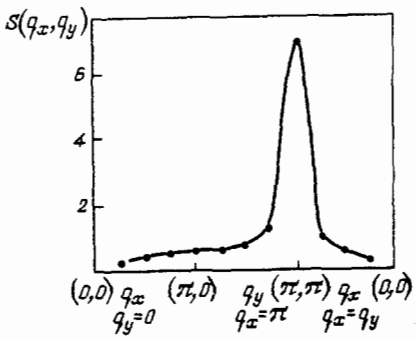


FIG. 8. Magnetic structure factor for the two-dimensional Hubbard model with $n = 1$, $U/t = 4$, $T = 6/t$ (Ref. 46).

is allowed to tend to infinity and the temperature to zero, i.e., whether there is a an incommensurable magnetic SDW phase for fillings other than half. The calculations cannot, however, be performed at low temperatures.

Long- or short-range antiferromagnetic order produces a radical change in the spectrum of electron states whose characteristics were calculated for two electron concentrations, namely, $n = 1$ and $n = 0.5$. One of the characteristics of single-particle states is the particle momentum distribution $n_\mathbf{k}$. This was found by direct evaluation of the single-particle temperature Green's function

$$G_{ij}(\tau) = -\langle Tc_i(\tau)c_j^+(0)\rangle \tag{4.7}$$

using the well known relation[18]

$$n_\mathbf{k} = T\sum_n e^{-i\omega_n\tau}G(\mathbf{k}, i\omega_n) \quad (\tau \to 0).$$

The results are shown in Fig. 9 (dotted lines). The solid curves in this figure show the Fermi distribution function for noninteracting particles

$$f(\varepsilon_\mathbf{k}) = \left(\exp\frac{\varepsilon_\mathbf{k} - \mu}{T} + 1\right)^{-1},$$

where the chemical potential $\mu$ is obtained from the condition that $n$ must be equal to 1 or 0.5. It is clear that the distribution has a Fermi-like character, but is quite different from the free-particle distribution, especially at half-filling. This difference is due to the appearance of the gap on the Fermi surface due to magnetic order. Actually, for $n = 1$ in the mean-field approximation, we have the following particle momentum distribution in the SDW state:

$$n_\mathbf{k} = \frac{1}{2}\left(1 - \frac{\varepsilon_\mathbf{k}}{E_\mathbf{k}}\right), \quad E_\mathbf{k} = \left(\varepsilon_\mathbf{k}^2 + \Delta^2\right)^{1/2}. \tag{4.8}$$

For the parameter values corresponding to Fig. 9, the gap equation (3.6) shows that $\Delta = 1.38t$ for which (4.8) gives the distribution $n_\mathbf{k}$ that is in good agreement with the QMCM calculations.

At the same time, when $n = 0.5$, the system does not have a well-defined magnetic structure factor, so that (4.8) cannot be applied to this case. The distribution $n_\mathbf{k}$ might be obtained by considering the correction to the electron self-energy due to the Coulomb interaction, using perturbation

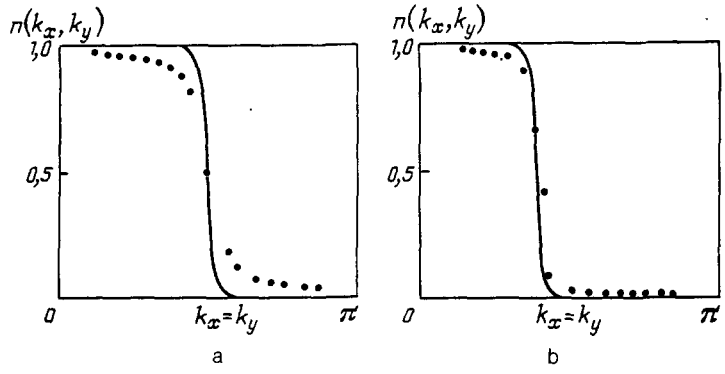


FIG. 9. Particle momentum distribution for $n = 1$ (a) $n = 0.5$ (b) $U/t = 4$, $T = t/6$ (Ref. 46).

theory. In the lowest order in $U$, the correction

$$\Sigma = \quad (4.9)$$

leads to very good agreement with the QMCM data shown in Fig. 9. This shows that when the band filling is very different from 1/2, there appears to be a Fermi liquid state. More direct information on this is provided by direct self-energy calculations using the formula

$$\Sigma(\mathbf{k}, i\omega_n) = G^{-1}(\mathbf{k}, i\omega_n) - i\omega_n + \varepsilon_{\mathbf{k}} - \mu, \quad (4.10)$$

where the Green's function $G(\mathbf{k},i\omega_n)$ is found numerically by the QMCM method. The imaginary part of $\Sigma$ that gives the structure density of single-particle states is shown in Fig. 10.

It is clear that a gap appears on the Fermi surface at half-filling due to antiferromagnetic order in the ground state. Let us compare this result with perturbation theory predictions. In the mean-field approximation,[22]

$$\Sigma(\mathbf{k}, i\omega_n) = \frac{\Delta^2}{i\omega_n + \varepsilon_{\mathbf{k}}}. \quad (4.11)$$

If we now place the vector $\mathbf{k}$ on the Fermi surface, we have $\varepsilon_{\mathbf{k}} = 0$ for $n = 1$, so that $\mathrm{Im}\,\Sigma(\mathbf{k}_F,i\omega_n) = -\Delta^2/\omega_n$. It is precisely this type of relation that is produced by the QMCM calculations. On the other hand, well away from half-filling, the behavior corresponds to the usual Fermi liquid: the frequency dependence of $\mathrm{Im}\,\Sigma(\mathbf{k}_F,i\omega_n)$ has a negative slope on the Fermi surface (see Fig. 10b). The calculated curve is in good qualitative agreement with perturbation-theory calculations that include only the correction (4.9).

It follows that QMCM calculations of $n_{\mathbf{k}}$ and $\mathrm{Im}\,\Sigma(\mathbf{k},i\omega_n)$ confirm the presence of a gap on the Fermi surface at half-filling, whereas well away from half-filling ($n = 0.5$), the system behaves as an ordinary Fermi liquid and is characterized by a Fermi surface. For $n = 0.87$ there is also no trace of a gap in the spectrum. Figure 11 shows the particle momentum distribution for a $16\times16$ lattice. The black squares represent the k-points for which $n_{\mathbf{k}} > 0.5$ with $U/t = 4$, $T = t/6$. The solid line drawn through these points represents the Fermi surface for noninteracting electrons ($U = 0$) with $n = 0.87$. Hence it is clear that, for a small deviation from half-filling, the system behaves like a Fermi liquid. Unfortunately, the QMCM calculations have been confined to moderate values of $U/t$ ($U/t = 4$). They show that the result obtained in the mean-field approximation for the gap and the particle momentum distribution, using perturbation theory in the parameter $U/t$, are in satisfactory agreement with numerical calculations. However, for very strongly correlated systems ($U \gg t$), this is still an open question. Moreover, the above calculations were performed for relatively high temperatures ($T = W/48$) because QMCM is difficult to implement at lower temperatures.

A short paper[47] presents a new numerical method for the investigation of the two-dimensional Hubbard model. The method is based on the evaluation of the energy functional of the system, using a particular approximation that ensures that the particle number, energy, momentum, and other variables are microscopically conserved. The different correlation functions are then calculated by variational differentiation with respect to external potentials. The authors of Ref. 47 maintain that the method can be used to examine large cluster systems and at low temperatures. By using stan-

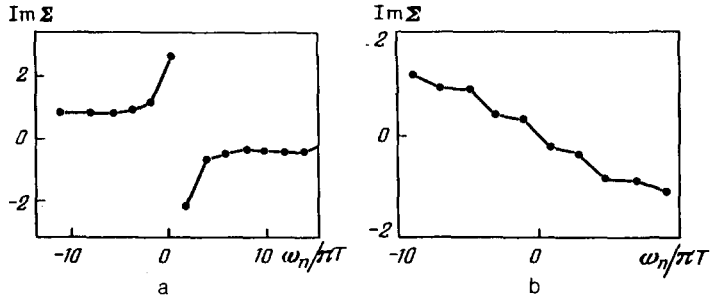


FIG. 10. Imaginary part of the self-energy as a function of frequency for (a) $n = 1$, $\mathbf{k}_F = (\pi/2,\pi/2)$, $\mathbf{k}_F = (0,\pi)$, (b) $n = 0.5$, $\mathbf{k}_F = (\pi/4,\pi/2)$. Parameter values: $U/t = 4$, $T = t/12$ (Ref. 46).

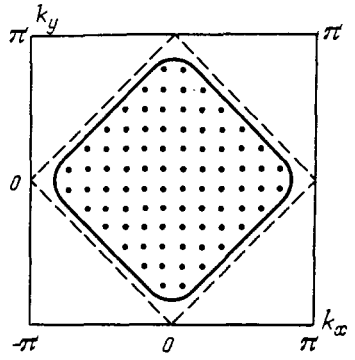


FIG. 11. Particle momentum distribution for a $16\times16$ lattice with $n = 0.87$, $U/t = 4$, $T = t/6$. Dashed line shows the Fermi surface for non-interacting electrons with $n = 1$ (Ref. 46).

dard results for the effective interaction between holes via spin and charge fluctuations to calculate the energy, these authors succeeded in constructing the phase diagram on the hole concentration versus temperature plane. We note that the antiferromagnetic state appears near half-filling for hole concentrations $n_h < 0.06$ whereas for $0.06 < n_h < 0.18$ there is a superconducting state with d-wave symmetry (for $U/t = 4$). The maximum $T_c$ is of the order of $0.01t$ which amounts to 15 K for an initial band width $8t = 1$ eV. This type of phase diagram occurs in model high-temperature superconductors in which superconductivity exists outside the region of antiferromagnetic order, but in the immediate proximity to it.

Another interesting result reported in Ref. 47 is the frequency dependence of the imaginary part of the magnetic susceptibility, which was used to find the dispersion law for spin excitations (paramagnons). Their velocity in the $\langle 11\rangle$ direction is of the order of $0.35ta$ which amounts to $1.4t$ Å for lattice constant $a = 4$ Å.

A similar phase diagram is reproduced in the detailed investigation reported in Ref. 48. It is shown there that the inclusion of parquet diagrams leads to quantitative agreement with the numerical QMCM results for intermediate values of $U/t$.

## II. APPROACH FROM THE SIDE OF LIMITING STRONG COULOMB INTERACTION

### 5. THE $t-J$ MODEL IN THE GENERALIZED RANDOM-PHASE APPROXIMATION

#### 5.1. Magnetic states in the $t-J$ model

One of the main manifestations of electron correlations under the conditions of strong Coulomb repulsion ($U \gg t$) is the splitting of the initial electron band into two Hubbard sub-bands, where the lower sub-band is associated with single-particle states and the upper with two-particle states of 'pairs' on single sites. The separation between them is of the order of $U$, so that at half-filling or less than half-filling ($n < 1$), the upper band can be neglected. The spectrum of electrons in the lower band (in the paramagnetic phase) in the limit as $U \to \infty$ is then determined by quasiparticle energies $[1 - (n/2)]\varepsilon_k$ where the factor $1 - (n/2)$ represents correlational band narrowing. This result is approximate and is probably interpolational in character. The corresponding approximation is referred to as Hubbard-I.[6]

For strongly correlated systems ($U \gg t$), regular perturbation theory should be constructed in the parameter $t/U$, i.e., the Coulomb interaction on a site should be included in the zero-order Hamiltonian, with the kinetic energy treated as a perturbation. The most convenient dynamic variables in this situation are the Hubbard operators[6] describing transitions between possible electron states on a given site. For example, the $t-J$ three-term model Hamiltonian $\mathscr{H} = \mathscr{H}_0 + \mathscr{H}_{kin} + \mathscr{H}_{eff}$ is then written in the form

$$\mathscr{H}_{kin} = t\sum_{i,\Delta,\sigma} X_i^{\sigma 0} X_{i+\Delta}^{0\sigma}, \tag{5.1}$$

$$\mathscr{H}_{eff} = J\sum_{i\Delta} (X_i^{-+} X_{i+\Delta}^{+-} - X_i^{++} X_{i+\Delta}^{--}), \tag{5.2}$$

and the single-site energy $\mathscr{H}_0$ is a linear form in the Hubbard operators.

Since there is a Wick theorem for Hubbard operators, we can construct for the Hubbard model a perturbation theory in the form of a diagram technique (the most complete description of this is given in Ref. 7). In the case of the $t-J$ model, when the perturbation is taken to be $\mathscr{H}_{int} = \mathscr{H}_{kin} + \mathscr{H}_{eff}$, this procedure is a special combination of the diagram technique for Fermi systems and for spin operators.[7] Its elements are the fermion Green's function $G_\sigma(k)$ (they will be represented by solid lines with white and black arrows representing the spin projections) and boson Green's functions $D(k)$ represented by broken lines. Wavy and dotted lines represent the 'interactions'

$$\varepsilon_k = t\sum_{\vec{\Delta}} e^{i\mathbf{k}\vec{\Delta}}, \quad J(\mathbf{k}) = \sum_{\vec{\Delta}} e^{i\mathbf{k}\vec{\Delta}}. \tag{5.3}$$

In standard perturbation theory in the small parameter $U/t$, which is employed in Part I, we widely use the random-phase approximation that involves the summation of loop diagrams. The generalized random-phase approximation (GRPA) was proposed in Ref. 12 for the $t-J$ model. As in the case of small $U/t$, here again we sum all the possible loop diagrams of which there are four types, namely,

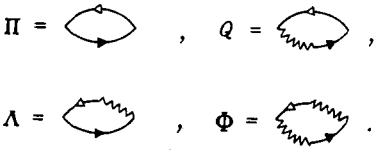


(5.4)

The fermion lines correspond to the electron Green's functions in the Hubbard-I approximation:

$$G_\sigma^0(k) = \frac{1}{i\omega_n - E(\mathbf{k})}, \quad E(\mathbf{k}) = \left(1 - \frac{n}{2}\right)\varepsilon_k - \mu. \tag{5.5}$$

In the GRPA approximation, the magnetic susceptibility of the paramagnetic phase is given by[12]

$$\chi(k) = \frac{\chi_0(k)}{(1 - \Lambda(k))(1 - Q(k)) + \chi_0(k)(\Phi(k) + J(k))}, \tag{5.6}$$

where the 'bare' susceptibility contains localized and collective contributions

$$\chi_0(k) = \frac{nn_0}{T}\delta_{\omega_n,0} - \Pi(\mathbf{k}, i\omega_n). \tag{5.7}$$

The factor $n_0$ depends on the ratio $\mu/T$, where $n_0 = 0$ for $T = 0$ and $n < n_c$, and $n_0 = 1$ for $n > n_c$, where $n_c$ is the critical concentration for which localized magnetic moments appear in the system. It is found that the chemical potential $\mu$ changes sign at this point. It is possible that this approximation, which leads to a much too rapid variation in $n_0$, is too coarse, but the result given by (5.6) and (5.7) shows that there is a crossover in the system from itinerant to localized magnetism. We therefore conclude that for $n < n_c$, the system behaves as an itinerant magnet whereas for $n > n_c$ it displays simultaneously the properties of itinerant and localized magnets. In (5.7) this corresponds to two contributions to the magnetic susceptibility, namely, the Curie–Weiss and the Pauli contributions.

Analysis of (5.6) for the three-dimensional case leads to the magnetic phase diagram shown in Fig. 12. The antiferromagnetic phase A is characterized by the vector $\mathbf{k}_0 = (\pi,\pi,\pi)$; it occurs for large enough values of the effective exchange integral and in the concentration interval adjacent to the $n = 1$ edge. We note that, at the point of intersection of the ferro- and antiferromagnetic instability lines, we should take into account the interaction between order parameters, which modifies the phase diagram in the neighborhood of this point.

### 5.2. Cooper pairing via spin fluctuations in the paramagnetic phase

The effective interaction between electrons in the singlet channel is described by the following contributions in the GRPA approximation:

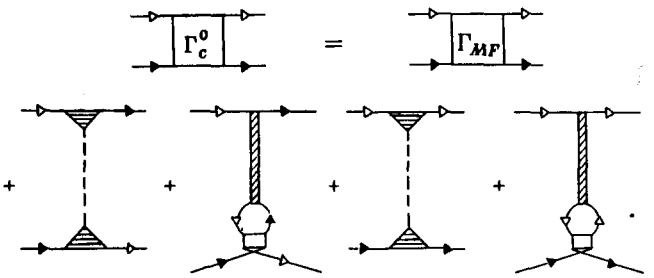


(5.8)

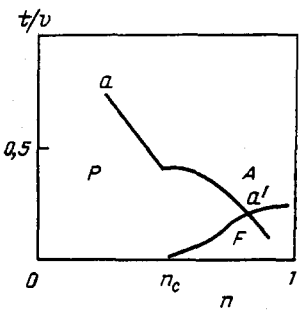


FIG. 12. Magnetic phase diagram for the three-dimensional $t - J$ model on the $(t/U,n)$ plane with $T = 0$ (Ref. 12). The diagram shows the para ($P$), ferro ($F$), and antiferro ($A$) phases.

The last four graphs describe interactions via spin fluctuations with spin flip (first pair of graphs) and with spin conservation (second pair). The shaded four-particle and three-particle vertex parts are taken in the GRPA approximation, i.e., they are represented by chains made up of the loops in (5.4). The dashed line in the first and third graphs, represents the transverse and longitudinal spin Green's functions. Finally, the first graph in the first part represents the bare interaction corresponding to the Hamiltonian $\mathscr{H}_{\text{kin}} + \mathscr{H}_{\text{eff}}$:

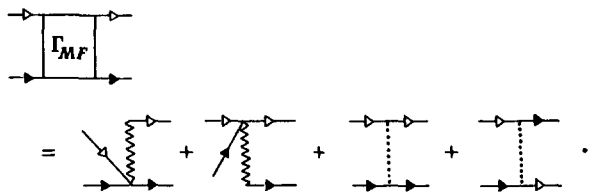


(5.9)

At the same time, we must write down the self-energy part due to the interaction with spin fluctuations. For example, for an electron with spin ↑,

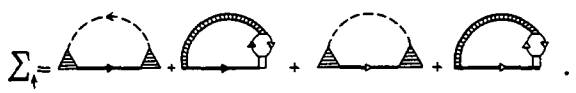


(5.10)

There is a definite correspondence between the expressions for $\Gamma_c^0$ given by (5.8) and (5.10) and expressions (2.9) and (2.16) describing the situation with $U \ll t$. In the case of strong correlation, there are two additional graphs in the expressions for $\Gamma_c^0$ and $\Sigma$ that are due to the appearance in the system of localized spin states [first and third graphs in (5.8) and (5.10)]. The remaining pair of graphs (second and fourth) represents the interaction between electrons via fluctuations in the itinerant states. It is precisely this type of graph that is present in the theory of superconductivity in itinerant magnets.[2] Spin fluctuations in such systems (paramagnons) mediate the interaction between electrons. The shaded lines in the second and fourth graphs in (5.8) and (5.10) correspond to the paramagnon propagator. The essential difference between the systems with strong and weak Coulomb interactions is still the type of bare vertices. Thus, in the procedure involving the Hubbard operators, we have vertices with three fermion lines [cf. the expression given by (5.9)], which is typical for all systems described by operators for which the commutator or anticommutator is not a $C$-number.

We must now construct the equation for $\Gamma_c$ in the Cooper channel, using the bare vertex $\Gamma_c^0$. This has the same form as (2.15) that we first encountered in the theory with weak Coulomb interaction. In the graphs of (5.8) and (5.10), the thick intermediate lines correspond to the renormalized Green's function (2.18) where $E(\mathbf{k})$ now represents the energy of the electron in the lower Hubbard band [see (5.5)]. We thus arrive at two coupled equations for $Z(k)$ and $\varphi(k)$ (the latter represents the vertex part in the Cooper channel) that have the standard form of the equations of the theory of superconductivity with strong coupling, i.e., (2.19) and (2.20). In this case, the pairing inter-

action $V$ and the total interaction $V_z$ consist of two contributions[50]

$$V_z = V_m + V_c, \quad V = -V_m + V_c,$$

where

$$V_m(\mathbf{kk}', i\omega_n - i\omega_{n'}) = \frac{3}{2}\frac{\varepsilon_k^2\chi_0 - \varepsilon_{k'}(2-\Lambda-Q) - (\Phi+J)}{(1-\Lambda)(1-Q)+\chi_0(\Phi+J)}, \tag{5.11}$$

$$V_c(\mathbf{kk}', i\omega_n - i\omega_{n'}) = \frac{1}{2}\frac{\varepsilon_k^2\chi_0^c + \varepsilon_{k'}(2+\Lambda+Q) - (\Phi-J)}{(1+\Lambda)(1+Q)+\chi_0^c(\Phi-J)}. \tag{5.12}$$

All the quantities in (5.11) and (5.12) are evaluated for the argument $k - k'$.

The denominator in (5.11) is identical with the denominator in the expression for the magnetic susceptibility, and the entire expression for $V_m$ must be treated as the contribution to the effective interaction due to magnetic fluctuations whereas $V_c$ is the contribution due to charge fluctuations in the system. The quantity $\chi_0^c(k)$ is the initial dielectric susceptibility and $V_c$ in (5.12) is equal to the denominator of the dielectric susceptibility. The charge term can be neglected near the boundary of the phase transition to the magnetically ordered state, so that $V_z = V_m$ and $V = -V_m$. Since the strong interaction must be positive, we see that the 'pairing' part of the interaction mediated by the magnetic fluctuations is in fact repulsive, as in the case of the weak Coulomb interaction.

It is shown in Ref. 2 that an anisotropic superconducting order parameter can appear in the repulsive pairing potential when $U \ll t$. It can be shown that this can also occur for $U \gg t$ although the situation is then much more complicated because localized magnetic moments are present in the system.

The integral equations given by (2.19) and (2.20) with the kernels (5.11) and (5.12) are very difficult to treat analytically. We shall therefore confine ourselves to the simplest situation that will enable us to establish the basic tendencies in the structure of the solutions. In particular, we shall examine the weak-coupling limit by analogy with the electron-phonon model of superconductivity.

First, we note that the expression for $\chi_0(\mathbf{k}, i\omega_n)$ contains the quasiparticle term $\sim\delta_{\omega_n,0}$ associated with localized magnetic moments. The effective interaction must therefore also contain the quasistatic and dynamic contributions, which we shall denote by $V^{st}$ and $V^{dyn}$. The latter is due to itinerant states. The static contribution can be readily separated out in (5.11) and (5.12). If we suppose that the Fermi liquid picture is valid for our system, then the equations for $Z$ and $\varphi$ can be averaged over the Fermi surface. We then obtain the following equation for $T_c$ in the intermediate coupling limit:

$$\ln\frac{T_c}{T_{c0}} = \psi\left(\frac{1}{2}\right) - \psi\left(\frac{1}{2}+\rho\right), \tag{5.13}$$

where

$$T_{c0} = \frac{2\gamma}{\pi}\omega_m \exp\left[-\frac{1-(n/2)+\lambda_z}{\lambda_l}\right], \tag{5.14}$$

$$\rho = \frac{1}{2}\frac{\eta_z - \eta_l}{1-(n/2)+\lambda_z}; \tag{5.15}$$

in which, as before, $\omega_m$ is the limiting frequency of the spin-fluctuation spectrum, $\lambda_z$, $\lambda_l$, $\eta_z$, $\eta_l$ represent the effective interactions at zero frequency, averaged over the Fermi surface and given by

$$\lambda_z = \langle\langle V_z^{dyn}(\mathbf{kk}', 0)\rangle\rangle_\rho, \quad \lambda_l = \langle\langle \psi_l(\mathbf{k}) V^{dyn}(\mathbf{kk}', 0)\psi_l(\mathbf{k}')\rangle\rangle_{\rho_l}, \tag{5.16}$$

$$\eta_z = \langle\langle V_z^{st}(\mathbf{kk}', 0)\rangle\rangle_\rho, \quad \eta_l = \langle\langle \psi_l(\mathbf{k}) V^{st}(\mathbf{kk}', 0)\psi_l(\mathbf{k}')\rangle\rangle_{\rho_l}, \tag{5.17}$$

in which $\langle\langle ... \rangle\rangle$ represents averaging over momenta $\mathbf{k}$ and $\mathbf{k}'$, and $\lambda_l$ and $\eta_l$ are coupling constants for the superconducting order parameter with $l$-wave symmetry when the solution of the equation for $\varphi(k)$ is sought in the form of (2.23). The separation of the interactions (5.11) and (5.12) into $V^{st}$ and $V^{dyn}$ can be readily achieved by using (5.7) for $\chi_0$.

The formulas given by (5.13) and (5.14) are meaningful only if $\lambda_l > 0$ (the total coupling constant $\lambda$ is always positive). The coupling constant $\lambda$ then determines the superconducting transition temperature due to pairing mediated by dynamic spin fluctuations. Equation (5.13) has the same form as the corresponding equation for superconductors with magnetic impurities[5] and describes pairing due to the appearance of localized magnetic moments for $n > n_c$ when $\eta_z$ and $\eta_l$ are nonzero. In the case of itinerant magnetism ($n > n_c$), the parameters $\eta_z$ and $\eta_l$ vanish identically, and $T_c$ is given by (5.14).

We thus see that the most favorable conditions for the existence of a superconducting state in the $t-J$ model (in the paramagnetic phase of a metal!) are realized in the case of itinerant magnetism ($n < n_c$) near the antiferromagnetic instability line (line $a$ in Fig. 12). As for $U \ll t$, and despite the repulsive nature of the electron interaction mediated by spin fluctuations, the quantity $\lambda_l$ can be positive near this line when the order parameter has d-wave symmetry. However, the corresponding concentration interval lies well away from half-filling, and it is precisely this region that is relevant for the description of practical high-$T_c$ materials. Since an antiferromagnetic state appears in the $t-J$ model for $n > n_c$ (this is already clear from the phase diagram of Fig. 12, obtained in GRPA approximation), the present problem is to investigate the possibility of a superconducting state in the antiferromagnetic phase. We saw in Section 3 that, in the case of a weak Coulomb interaction, the pairing potential mediated by spin fluctuations gives rise to a much stronger potential in the antiferromagnetic phase as a result of the spin-correlation mechanism. The immediate problem for the theory of strongly correlated systems is that of a hole (magnetic polaron) in an antiferromagnetic matrix in the

context of the $t-J$ model, followed by an examination of the pairing hole interaction mediated by magnetic fluctuations.

We now return to the main topic of this Section and note that the matrix element (5.11) of the effective interaction between electrons mediated by spin degrees of freedom corresponds in the lowest-order approximation to the so-called kinematic pairing[52,53] (see also Ref. 54). This mechanism arises when we retain only the first graph in the expression for the effective interaction (5.8) and discard all other terms that give an interaction mediated by fluctuations. It is clear from (5.11) that, in this approximation, a pairing potential arises for $n > n_c$. However, fluctuations produce a greater renormalization of this potential and suppress superconductivity by the parallel mechanism of pairing by localized magnetic moments, which is turned on precisely for $n > n_c$. The same conclusion about the kinematic interaction is reported in Ref. 55.

## 6. A HOLE IN THE $t-J$ MODEL WITH ANTIFERROMAGNETIC ORDER

### 6.1. Qualitative picture in the Ising limit

Well before the recent publications on the motion of a hole in the antiferromagnetic state of a strongly correlated system, there were three papers[56–58] that provided a fundamental contribution to our understanding of this problem. They examined the state of a hole in a Néel antiferromagnet described by the $t-J$ model in the Ising approximation for the exchange-interaction Hamiltonian. A qualitative analysis of the motion of a hole, which we investigated in Section 1 in connection with the dynamics of a hole pair in a two-dimensional antiferromagnetic matrix (see Fig. 1), was first given in Ref. 57. The motion of a hole in a two-sublattice three-dimensional Néel antiferromagnet is always accompanied by an irregular distribution of spins along its trajectory, which requires the expenditure of energy $\sim Jl$ where $l$ is the length of the trajectory. The motion of the hole is thus energetically unfavorable, and it becomes auto-localized. The auto-localization center of the hole (or extra electron) is the site occupied by the hole for which the ideal antiferromagnetic distribution of spins is preserved. This state is the analog of the three-dimensional oscillator formed by the particle moving not in the usual quadratic potential but in a linear potential. A bound state with energy $\sim (J_z/t)^{2/3}t$, measured from the bottom of the band, is formed in this potential. The quasi-oscillator state is significantly different from the polaron state in which the deformation of the antiferromagnetic structure is transported by the hole (or electron) throughout the lattice, even when the effective mass is high. In the quasi-oscillator state, the resulting local deformation of magnetic structure is not transported over the lattice if we do not introduce the transverse spin components in the Heisenberg exchange-Hamiltonian. These components allow processes involving spontaneous spin flip, so that the deformation of the structure can relax and the motion of a hole is allowed.

The translational motion of a hole is therefore impossible in the Ising limit (the effective mass is infinite) and the spectral density of a hole, $A(\mathbf{k},\omega)$, with a certain fixed wave vector $\mathbf{k}$ does not have a quasiparticle peak signaling a coherent state of the hole. The spectral density corresponding to the hole has an incoherent character.[58] More precisely, it is shown in Ref. 58 that the antiferromagnetic state at exact half-filling ($n = 1$) has the density of correlated single-particle states occupying the energy band between $-w_0 zt$ and $w_0 zt$ where $w_0 \approx 0.75$. We thus have a 25% correlational narrowing of the original band ($-zt, zt$). The introduction of the hole produces a spreading of the lower edge of this band, i.e., a tail on the density of states that is typical for the theory of impurities in a metal.[59] This tail corresponds to the incoherent contribution to $A(\mathbf{k},\omega)$ that arises from the interaction between the hole and magnetic order fluctuations.

The above quasi-oscillator picture is corrected in Ref. 62. It is found that if the hole executes a loop and hops over neighboring sites forming a square cell of two-dimensional lattice (see Fig. 1), and if it runs around it one and a half times, then it ends at the opposite end of the diagonal of the square, so that no changes are produced in the antiferromagnetic lattice. This means that the hole can move over the magnetic lattice without losing energy by lattice deformation. The contribution of this type of trajectory (Trugman loop) obviously leads to a finite hole mobility even in the Ising limit.

As already noted, the introduction of transverse spin components leads to finite hole mobility. The effective mass of a hole is determined by scattering by spin fluctuations (spin waves). At low temperatures, only the emission of low-energy spin waves is possible. If the density of states in the spectrum of low-energy spin excitations is low, we may expect the presence of well-defined coherent states of holes as quasiparticles near the bottom of the hole spectrum, with finite but not too short lifetimes. There is more scattering at higher energies, and the quasiparticle peak broadens. The self-consistent theory of the quasiparticle state of a hole was developed in Ref. 44 in which it was shown that a quasiparticle peak in the spectral density $A(\mathbf{k},\omega)$ is present in the two-dimensional model. This paper, which will be examined in detail below, was preceded by studies of one-dimensional[60] and two-dimensional[61,62] models.

### 6.2. Self-consistent theory of the quasiparticle state

To include the Ising limit in the theory that we have just examined qualitatively, let us consider the anisotropic model with two exchange parameters, namely, $J_z$ (for the term $S_i^z S_j^z$) and $J_\perp$ (for the transverse spin components). We now introduce the corresponding changes into the exchange part of the Hamiltonian (1.2) for the $t-J$ model, and also neglect the Coulomb term. Consider the system at half-filling (Néel ground state) into which one hole has been introduced. To find the principal characteristics of the hole interacting with spin fluctuations, we construct the effective Hamiltonian $\mathscr{H} = \mathscr{H}_0 + \mathscr{H}_{\text{int}}$ where $\mathscr{H}_0$ is the spin-wave term and $\mathscr{H}_{\text{int}}$ describes the interaction of the hole with spin waves[44]

$$\mathscr{H}_0 = \sum_{\mathbf{q}} E_{\mathbf{q}} \beta_{\mathbf{q}}^+ \beta_{\mathbf{q}}, \tag{6.1}$$

$$\mathscr{H}_{\text{int}} = -zt \sum_{\mathbf{k},\mathbf{q}} f_{\mathbf{k}} f_{\mathbf{k}-\mathbf{q}}^+ (u_{\mathbf{q}} \gamma_{\mathbf{k}-\mathbf{q}} \beta_{\mathbf{q}} + v_{\mathbf{q}} \gamma_{\mathbf{k}}^+ \beta_{-\mathbf{q}}^+) + \text{c.c.} \tag{6.2}$$

where $\beta_{\mathbf{q}}$ is the Bose magnon anihilation operator, $f_{\mathbf{k}}$ is the Fermi hole anihilation operator, $E_{\mathbf{q}}$ is the magnon energy,

and $u_q$ and $v_q$ are the coefficients of the transformation that diagonalizes the exchange Hamiltonian in the spin-wave approximation. We have

$$E_q = zJ_z\left(1-\alpha^2\gamma_q^2\right)^{1/2}, \quad \gamma_q = \frac{1}{z}\sum_{\vec{\Delta}} e^{i\mathbf{q}\vec{\Delta}},$$

$$u_q^2 = \frac{1}{2}\left[1+\frac{1}{(1-\alpha^2\gamma_q^2)^{1/2}}\right], \quad v_q^2 = \frac{1}{2}\left[1-\frac{1}{(1-\alpha^2\gamma_q^2)^{1/2}}\right],$$

where $\alpha = J_\perp/J_z$ is the exchange anisotropy parameter. The effective Hamiltonian (6.1)–(6.2) arises from the following representation of the initial Fermi operators $c_{i\sigma}^+$ in terms of the auxiliary Fermion operator $f_i$ and the boson operator $b_{i\sigma}^+$: $c_{i\sigma}^+ = f_i b_{i\sigma}^+$.

Let us now examine the Green's function $G(\mathbf{k},\omega)$ of a hole, constructed from the operators $f_i$ and $f_i^+$. In the spirit of the approximations that we have already used many times, we take the self-energy part in the form

$\Sigma =$  , (6.3)

where the double solid line is the self-consistent hole Green's function and the double dashed line is the spin-wave Green's function. This means that, in the approximation defined by (6.3), we neglect the renormalization of vertex parts of the hole-magnon interaction (6.2). The Green's function is thus determined from the corresponding self-consistent integral equation

$$G(\mathbf{k},\omega) = \frac{1}{\omega - \sum_{\mathbf{q}} f(\mathbf{k},\mathbf{q})G(\mathbf{k}-\mathbf{q},\omega-E_q)}, \tag{6.4}$$

where the square of the amplitude of the electronmagnon interaction is given by

$$f(\mathbf{k},\mathbf{q}) = z^2t^2|\gamma_{\mathbf{k}-\mathbf{q}}u_q + \gamma_{\mathbf{k}}v_q|^2. \tag{6.5}$$

The quasiparticle properties of a hole are determined by the size of the pole contribution to the Green's function which we write in the form

$$G(\mathbf{k},\omega) = \frac{a_{\mathbf{k}}}{\omega-\omega_{\mathbf{k}}} + G_{\text{inc}}(\mathbf{k},\omega), \tag{6.6}$$

where the second term represents the incoherent state. The pole $\omega_{\mathbf{k}}$ is found from the equation

$$\omega_{\mathbf{k}} = \Sigma(\mathbf{k},\omega_{\mathbf{k}}), \tag{6.7}$$

and the residue at the pole $a_{\mathbf{k}}$ is given by (4.8) which can be written in the form

$$a_{\mathbf{k}} = \frac{1}{1+\int d\varepsilon \frac{\Gamma(\mathbf{k},\varepsilon)}{(\varepsilon-\omega_{\mathbf{k}})^2}}, \tag{6.8}$$

in which we use the dispersion relation between Re $\Sigma$ and Im $\Sigma$ where $\Gamma(\mathbf{k},\varepsilon) = (1/\pi)\,\text{Im}\,\Sigma(\mathbf{k},\varepsilon)$.

In the Ising limit ($\alpha\to 0$), equations (4.4) and (4.5) give $a_{\mathbf{k}}\to 0$, i.e., there are no quasiparticle states, which means that this spectrum is incoherent.[44] For finite but small $\alpha$, all the quantities can be expanded in powers of $\alpha \ll 1$, and this leads to the following estimates for the strength of the coherent state $a_{\mathbf{k}}$, the width $\delta W$ of the hole band, and the effective mass $m$ in the two-dimensional model:

$$a_{\mathbf{k}} \approx \frac{J_z}{t}, \quad \delta W \sim J_\perp, \quad m^* \approx \frac{t}{J_z}m. \tag{6.9}$$

Thus, even for $J_z \ll t$, there are hole quasiparticle states. They form a band near the beginning of the spectrum at about $-zt$, which has a width of the order of $J_\perp$. Most of the hole states are incoherent and the spectrum of these states extends over an energy interval of the order of $zt$ above the band of quasiparticle states.

We now turn to the isotropic case ($\alpha = 1$) for which $J_z = J_\perp \equiv J$. There is no gap in the spectrum of spin excitations. Low-energy excitations have an imaginary dispersion law, so that, in the two-dimensional case, the density of states in the spin-wave spectrum is also an imaginary function of energy. The result of this is that the scattering of the hole by spin waves does not destroy the quasiparticle state. At high hole energies ($\omega \gtrsim J$), the large number of spin excitations ensures that the hole spectrum becomes incoherent. It is clear from these considerations that for hole energies $\omega \lesssim J$ we may suppose that the pole contribution to the hole Green's function (4.6) will be predominant. We can then determine the residue $a_{\mathbf{k}}$ by substituting for $G(\mathbf{k},\omega)$ in (6.3) the expression given by (6.4) with $\Sigma$ replaced with its pole part. This leads to the inequality

$$a_{\mathbf{k}} \le \frac{1}{1+t^2\sum_{\mathbf{q}} f(\mathbf{k},\mathbf{q})\frac{a_{\mathbf{k}-\mathbf{q}}}{(\omega_{\mathbf{k}}-\omega_{\mathbf{k}-\mathbf{q}}-E_q)^2}}, \tag{6.10}$$

from which it follows that, for $D = 2$,

$$a_{\mathbf{k}} \lesssim \frac{J}{t}, \tag{6.11}$$

which confirms the existence of the quasiparticle peak. The consequence of this is that the incoherent part of the spectral function remains equal to a constant over a wide energy range of the order of $t$: $A(\mathbf{k},\omega) \approx 1/t$.

The above discussion thus shows that, for a two-dimensional Heisenberg antiferromagnet described by the $t-J$ model, the hole is a coherent quasiparticle with peak intensity $\sim J/t$. This peak is localized at approximately the edge of the original band $-zt(z=4)$ and its width is of the order of $J$. A band of incoherent states with a width of the order of $t$ lies just outside this peak.

### 6.3. Numerical calculations based on exact diagonalization

All these important theoretical predictions[57,58,61,62] require confirmation by numerical calculations because they rely on approximations that are not readily controlled. However, numerical studies of this problem are also very difficult. There are two main methods, namely, the Monte Carlo technique and exact diagonalization of the Hamiltonian. However, in the Monte Carlo method, it is difficult to examine low temperatures and sufficiently high impurity concentrations because of the 'sign problem' in the determinant for Fermi particles. These difficulties are not encountered in the exact diagonalization method, but in practice the method has to be confined to small clusters because the number of variables characterizing the state of a cluster increases exponentially with increasing number of particles ($3^N$ for the

$t-J$ model and $4^N$ for the Hubbard model). A complete calculation is therefore possible in the $t-J$ model for the $4\times4$ two-dimensional cluster.

The first publications reporting work by independent groups[63-64] on $4\times4$ clusters containing one hole confirmed many of the basic predictions of the theory such as the presence of the quasiparticle peak near the bottom of the hole spectrum, the wide band in the incoherent spectrum above this peak, and the high effective hole mass due to its interaction with magnetic order. Calculations showed that the quasiparticle peak appeared for moderate values of the parameter $J/t > J_c/t = 0.075$ (Ref. 67) for which the ideal system (in the absence of a hole) has an antiferromagnetic ground state; in the presence of a hole, the total spin of the state is $S^z = 1/2$. For lower values of $J/t$, the ground state of the cluster has spin $S^z = 15/2$, indicating the onset of saturated ferromagnetism in accordance with Nagaoka's theorem.[69] In the ferromagnetic state, the ground-state momentum (which can be ascribed to the hole) is $\mathbf{k} = 0$, whereas in the state with spin $S^z = 1/2$ the momentum is nonzero:

$$\mathbf{k} = (\pm\frac{\pi}{2}, \pm\frac{\pi}{2}), \quad \mathbf{k} = (\pi, 0), \quad \mathbf{k} = (0, \pi). \tag{6.12}$$

The degeneracy is probably due to the high symmetry of the cluster. It is remarkable that if we include only the Ising part of the interaction in the Heisenberg Hamiltonian, then the results are different: the ground state with spin $S^z = 1/2$ has momentum $\mathbf{k} = 0$. This means that quantum fluctuations due to the transverse spin components play a significant part in the behavior of a hole. We also note that the finite momentum of the ground state with $S^z = 1/2$ was obtained in Ref. 61 in the spin-wave approximation using the variational method.

The cluster dimensions were also varied in the publications cited above and it was shown that the main physical conclusions about cluster dimensions were stable, so that the data obtained for the small $4\times4$ cluster may well have been valid for an infinite system. The reason for this was that the perturbation of the antiferromagnetic matrix introduced by the hole was highly localized.

The most complete set of results was obtained in Ref. 70 which was also concerned with the $4\times4$ cluster with periodic boundary conditions. We shall now review some of the results of these calculations. First, we note that the hole spectral density $A(\mathbf{k},\omega)$ was calculated for a wide range of values of $J/t$. A typical spectrum is shown in Fig. 13. As $J/t$ increases, the main peak shifts to the right and its height increases. At the same time, the fine structure of the two different sets of points vanishes and only two low-intensity peaks remain. For $0.2 \leqslant J/t \leqslant 1.0$, the position of the first three peaks (I, II, III) varies with $J/t$ as follows:

$$\begin{aligned} &\text{I. } E_h = -3{,}17 + 2{,}83(J/t)^{\alpha}t, \quad \alpha = 0{,}73,\\ &\text{II. } E_h = -3{,}13 + 5{,}36(J/t)^{\alpha}t, \quad \alpha = 0{,}70,\\ &\text{III. } E_h = -3{,}23 + 6{,}26(J/t)^{\alpha}t, \quad \alpha = 0{,}63. \end{aligned} \tag{6.13}$$

For wave vectors $\mathbf{k} = (\pi/2,0)$, $(\pi,\pi/2)$, $(\pi,0)$, and $(0,0)$ we again have a power-type law with similar values of $\alpha < 1$.

This power-type dependence of peak position on $J/t$ may be due to discrete states of the hole in the linear potential (quasi-oscillator model[57]) when only the Ising part of the exchange interaction is taken into account. A discrete set of levels is then found to arise and is given by the eigenvalues of the Airy equation[44,57,61]

$$E_h = -2z^{1/2}t + a_n(J_z/t)^{2/3}t. \tag{6.14}$$

The first three values of $a_n$ (2.33, 4.08, and 5.52) are in good agreement with the coefficients of $(J/t)^{\alpha}$ in (6.13) and $\alpha \approx 2/3$. This is surprising because one would expect that the transverse part of the Heisenberg exchange should spread the potential well produced by the hole due to the Ising part. However, this does occur: comparison of calculations based on (6.13) with the theoretical formula (6.14) for the $t-J$ model shows good agreement at least for the first few levels of the quasi-oscillator. For $J_z = 0$, (6.14) gives the position of the lower edge of the quasiparticle spectrum as $-2z^{1/2}t$, which was obtained in Ref. 58 as the result of correlational narrowing of the band [it is shown in Ref. 44 that the factor $(z-1)^{1/2}$ in Ref. 58 should be replaced with $z^{1/2}$].

The width $\Gamma$ of the quasiparticle state corresponding to the first peak is practically a linear function of $J/t$:

$$\Gamma/t = -0{,}14 + 1{,}97(J/t)^{0{,}98}, \quad 0{,}1 \leq J/t \leq 0{,}4, \tag{6.15}$$

which agrees with theoretical calculations.[44,71] The peak height $a_{\mathbf{k}} \sim (J/t)^{0.5}$ differs from the prediction in Ref. 44, i.e., $a_{\mathbf{k}} \sim J/t$, but is in good agreement with the prediction reported in a recent paper.[71]

Summarizing the above results, we may conclude that numerical calculations confirm the quasiparticle properties of a hole in the $t-J$ model, as derived in Ref. 44. However, these calculations have not revealed an incoherent contribution to $A(\mathbf{k},\omega)$, although they have confirmed the Ising character of the quasi-oscillator state. Instead of the incoherent background, we obtain the fine structure of the spectrum. This result is unexpected because spin fluctuations in the Heisenberg model (spin waves) should on the face of it broaden all the closely spaced peaks and thus produce an incoherent background. It will therefore be necessary to verify these calculations for clusters larger than $4\times4$.

In conclusion, we present a calculation of the total density of states $\rho(\omega) = \Sigma_{\mathbf{k}} A(\mathbf{k},\omega)$ in the hole spectrum (Fig. 14). As can be seen, there is a well-defined fine structure. The peaks labeled I, II, and III correspond to contributions with the following wave vectors, respectively: $(\pi/2,\pi/2)$, $(\pi/2,\pi)$, $(\pi/2,0)$, $(0,0)$, and $(\pi,\pi)$. It is therefore difficult to speak of an incoherent hole spectrum if we judge this from the results obtained for a small cluster.

The same paper reported a study of the original Hub-

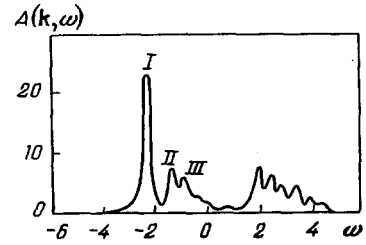


FIG. 13. Hole spectral density for $\mathbf{k} = (\pi/2,\pi/2)$ and $J/t = 0.2$ (Ref. 70).

bard model, using the exact diagonalization method. Because the number of states per site was large, the authors of this paper were forced to consider smaller clusters with $N = 8$ and 10. In the limit of large $U$, the results were found to be in qualitative agreement with numerical calculations based on the $t - J$ model. For moderate values of $U$, quasiparticle peaks were found near the bottom of the band of hole states.

Calculations based on exact diagonalization[7] are in good agreement with the Monte Carlo results[72] for intermediate values of $U$. Several papers have since appeared on this topic.[73-76]

### 6.4. Bound state of holes

Several authors[64,77,80] have succeeded in obtaining evidence for the formation of bound states of holes. The calculations were performed for $4\times4$ clusters containing several holes in different configurations. It was found that small hole separations were predominant, with holes forming bound states. This is not in itself surprising because an isolated hole disrupts four exchange bonds in the lattice. Consequently, for two nearest-neighbor holes there are seven broken bonds instead of the eight when the holes are at a large distance from one another. These results were confirmed by $8\times8$ calculations. When the hole concentration is high, energy minimization also leads to distributions for which the holes form an individual hole cluster.

The dynamic pair susceptibility of holes was investigated in Ref. 80 by considering the spectral density of the correlator $\langle \Delta_l^+(t)\Delta_l(0)\rangle$, where

$$\Delta_l^+ = \sum_{\mathbf{k}} \psi_l(\mathbf{k}) c_{\mathbf{k}\uparrow}^+ c_{\mathbf{Q}-\mathbf{k}\downarrow}^+$$

is the creation operator for a Cooper pair with $l$-wave symmetry. A sharp low-lying coherent peak with d-wave symmetry was shown by $4\times4$ calculations to be present for a wide range of values of $J/t$ in which the single-particle electron density of states also had a peak at the bottom of the Hubbard band. For p-wave symmetry, there was also a closely lying peak of lower intensity. However, the s-state behavior of the Cooper pair was different, i.e., there was no quasiparticle peak. Thus, at least for low hole concentrations, the s-type superconductivity was strongly suppressed and d-wave pairing predominated.

An unexpected result was obtained for clusters containing $N = 18$ and 20 particles in the case of moderate hole concentrations.[75] Two holes in such clusters correspond to concentrations $n_h = 10 - 15\%$. It was found that the Fermi surface (which separates points in $\mathbf{k}$-space with fillings $n_{\mathbf{k}}$ greater than and less than 1/2) does not have the form of hole pockets near the points $(\pi/2,\pi/2)$ and $(\pi/2,0)$. Instead, we have an electron-type Fermi surface whose size and shape are the same as for the surface for noninteracting electrons (Luttinger's theorem). These results are in agreement with Monte Carlo calculations using the Hubbard model with small $U$ (Ref. 46). Of course, it is impossible to exclude hole Fermi surfaces for low hole concentrations because the clusters have finite dimensions. For the same reason we cannot determine whether there is a jump in $n_{\mathbf{k}}$ on the Fermi surface, or the system is a marginal Fermi liquid.

Calculations have also shown that the excited states of a cluster fit into the excitation scheme for a Fermi liquid, i.e., there are hole-like and particle-like states with band width of the order of $J$ and effective mass $m^*/m \approx 1.5t/J$. Of course, these results do not show that the system has Fermi-liquid excited states because this would require us to show that the width of the single-particle peaks in the thermodynamic limit ($N\to\infty$) tends to zero as $\omega^2$ (or, at least as $\omega\ln\omega$ for the marginal Fermi liquid) when $\omega\to0$. Nevertheless, this leads us to hope that a strongly correlated system can be described by the Fermi liquid picture under certain specific conditions (for moderate hole concentrations). In particular, this would justify the use of this description in the superconductivity problem, as was done in Section 5.

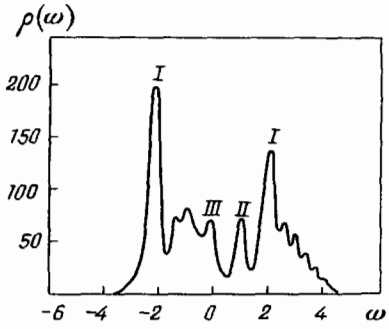


FIG. 14. The density of states in the $t - J$ model with one hole for $J/t = 0.2$ (Ref. 70).

## 7. CONCLUSION

Our main conclusion in this review is that, at present, the problem of the interaction between magnetic and superconducting states in the Hubbard model is far from solution despite the efforts of a large number of researchers working in this field (about 100 theoretical papers were published on this subject during the last two years). The problem is much more complicated than was believed at the beginning because a small parameter is not available in the most interesting region $U \sim W$ and because of the essentially many-particle character of the ground state near half-filling, although in the latter case there is small parameter, namely, the hole concentration. Nevertheless, examination of the two limiting cases $U \ll W$ and $U \gg W$ has led to a number of general conclusions.

(1) For both itinerant ($U \ll W$) and localized ($U \gg W$), magnetism it is possible to describe the antiferromagnetic state of the system near band half-filling. The mechanisms of magnetic instability are: nesting of the Fermi surface, which leads to the SDW-type long-range order for $U \ll W$ and indirect antiferromagnetic exchange, producing a Néel state for $U \gg W$. In both cases, a rise in the hole concentration is accompanied by a reduction in spin correlations, which is particularly dramatic in strongly correlated systems. A band appears in the electron spectrum in both cases because of the reduction in the translational symmetry of the system. Near half-filling, this gap falls on the Fermi level, giving rise to the insulating ground state.

These results correspond to the self-consistent field approximation. The simple picture is corrected when spin fluc-

tuations are taken into account. Fluctuations in longitudinal and transverse spin components in the state with broken symmetry lead to different effective spin interactions. These additional interactions produce a distortion of the SDW or Néel state. A helical phase appears in both limiting cases when there is a deviation from half-filling. Moreover, the stratification of the magnetic system into different phases[81–83] has been discussed for finite hole concentrations.

Numerical calculations performed for small clusters in the two-dimensional model reveal the magnetic-structure peak that corresponds, at least, to a well-defined short-range or long-range magnetic order. Such calculations also suggest the possibility of a periodic domain structure and other nonlinear structures such as vortices. It follows that the magnetic phase diagram in the Hubbard model is not as yet established near half-filling. All that can be said with certainty is that, at half-filling, the structure is antiferromagnetic, but may become distorted for a finite hole concentration. It appears that there are many magnetic phases with similar energies, which replace one another as the hole concentration increases.

(2) The indirect electron interaction mediated by spin fluctuations can lead to Cooper pairing. In the paramagnetic phase, the fluctuations produce a repulsion in the singlet channel. Despite this, there may be superconductivity with an anisotropic order parameter. Actually, in the case of cubic (square) lattice near antiferromagnetic instability, fluctuations give rise to Cooper pairing with d-wave symmetry in both cases, i.e., $U \ll W$ and $U \gg W$. However, in the latter case, localized magnetic moments appear in the system and give rise to pairing processes. It is then difficult to imagine high $T_c$ being produced by the spin fluctuations mechanism in the paramagnetic phase.

Near half-filling, longitudinal spin fluctuations in the antiferromagnetic phase give rise to the Cooper instability in the singlet channel, but transverse spin fluctuations (spin waves) produce a repulsion in this channel. As $U/W$ increases, the contribution of transverse fluctuations begins to predominate, and the superconducting state within the new antiferromagnetic phase should be replaced by the normal state with helical magnetic structure. It follows, that under certain definite conditions a superconducting state is possible in a magnetically-ordered phase (the most rigorous theory is based on the summation of parquet diagrams[84]), but a theory of the superconducting phase itself, that would enable us to calculate $T_c$, does not as yet exist. The most likely scenario is that high $T_c$ will be due to the magnetic fluctuation mechanism in regions with strong correlation ($U \gg W$) in which magnetic order is present. A magnetically ordered state (at least with short-range order) is essential to ensure that the pair breakdown mechanism is turned off on localized magnetic moments.

Numerical calculations for small clusters have, so far, led to contradictory results about Cooper pairing of holes.

(3) The most important component of the problem of magnetism and superconductivity in the Hubbard model near half-filling is the theory of the single-particle hole state. In the case of weak Coulomb interaction, $U \lesssim W$, analytic studies and numerical cluster calculations show that the hole is a well-defined quasiparticle with a clear coherent peak in the spectral density. We can therefore retain the Fermi liquid picture for finite hole concentrations.

For strongly correlated systems ($U \gg W$), a hole in the antiferromagnetic matrix can be described in terms of the quasi-oscillator, i.e., a particle that is auto-localized in the linear potential produced by a deformation of magnetic structure. This quasiparticle is mobile although it has a high effective mass. Its finite mobility is due to the transverse spin components in the exchange Hamiltonian (and also the contribution of states described by the Trugman loops). Numerical calculations performed for clusters confirm this picture, indicating the existence of a narrow coherent peak against the wide incoherent background in the spectral density of the single-particle state for a wide range of values of the parameter $U/W > 1$. The behavior of a collective of holes with finite hole concentration presents a very difficult problem. Cluster calculations show that, when $U/W$ is not too large, the Fermi liquid picture of the behavior of holes seems to be valid. However, it is not at all certain that it will continue to be valid for strongly correlated systems ($U \gg W$). This makes the theory particularly difficult in this limit.

A satisfactory theory of superconductivity in the Hubbard model near half-filling will have to await a more detailed study of the hole problem and of the interaction of holes, as well as the successful development of the magnetic phase diagram on the $W/U$, $n$ plane. This concludes our review of this very topical part of the theory of condensed matter. We emphasize once again that we have confined our attention to aspects associated with the assumption of a Néel ground state of the two-dimensional itinerant antiferromagnet, and have completely ignored the alternative possibility, namely, the RVB ground state.

In conclusion, we draw attention to a number of the most recent references on the problem under discussion.[86–97]


[1] N. F. Berk and J. R. Schrieffer, Phys. Rev. Lett. **17**, 433 (1966).
[2] D. J. Scalapino, E. Loh, and J. E. Hirsch, Phys. Rev. B **35**, 6694 (1987).
[3] S. V. Vonsovskiĭ and M. S. Svirskiĭ, Zh. Eksp. Teor. Fiz. **46**, 1619 (1964) [Sov. Phys. JETP **19**, 1095 (1964)].
[4] Yu. A. Izyumov and V. M. Laptev, Intern. J. Mod. Phys. **5**, 563 (1991).
[5] A. A. Abrikosov and L. P. Gor'kov, Zh. Eksp. Teor. Fiz. **39**, 1781 (1960) [Sov. Phys. JETP **12**, 1243 (1961)].
[6] J. Hubbard, Proc. R. Soc. London A **276**, 238 (1963); **277**, 237 (1964); **281**, 401 (1964).
[7] Yu. A. Izyumov and Yu. N. Skryabin, *Statistical Mechanics of Magnetically Ordered Systems* [in Russian], Nauka, M. 1987.
[8] A. V. Harris and R. V. Lange, Phys. Rev. **157**, 295 (1967).
[9] J. E. Hirsch, Phys. Rev. Lett. **54**, 1317 (1985).
[10] D. I. Khomskiĭ, Paper presented to a conference on problems in statistical physics held at Dubna, 1988 [in Russian].
[11] M. M. Mohan and N. Kumar, J. Phys. C **20**, L527 (1987).
[12] Yu. A. Izyumov and B. M. Letfulov, J. Phys.: Condens. Matter **2**, 8905 (1990).
[13] P. W. Anderson, Science **235**, 1196 (1987).
[14] Y. H. Chen, B. I. Halperin, F. Wilczek, and E. Witten, Intern. J. Mod. Phys. B **3**, 1001 (1989).
[15] Yu. A. Izyumov, N. M. Plakida, and Yu. N. Skryabin, Usp. Fiz. Nauk **159**, 621 (1989) [Sov. Phys. Usp. **32**, 1060 (1989)].
[16] T. Izuyama, D. Kim, and R. Kubo, J. Phys. Soc. Jpn. **18**, 1025 (1963).
[17] T. Moriya, *Spin Fluctuations in Itinerant Electron Magnetism*, Springer-Verlag, Berlin, 1985.
[18] A. A. Abrikosov, L. P. Gor'kov, and I. E. Dzyaloshinskii, *Methods of Quantum Field Theory in Statistical Physics*, Prentice-Hall, Englewood Cliffs, 1963 [Russ. original Nauka, M., 1962].
[19] V. L. Ginzburg and D. A. Kirzhnits, *Problems in High-$T_c$ Superconductivity* [in Russian], Nauka, M., 1977.
[20] H. Shimahava and S. Takada, J. Phys. Soc. Jpn. **57**, 1044 (1988).
[21] K. Yonemitsu, *ibid.*, **58**, 4576 (1989).
[22] J. R. Schrieffer, X. G. Wen, and S. C. Zhang, Phys. Rev. B **39**, 11663 (1989).
[23] D. M. Frenkel and W. Hanke, *ibid.*, **42**, 6711 (1990).

[24] H. Y. Chou and E. J. Mele, *ibid.*, **39**, 2956 (1989).
[25] Z. Y. Weng, T. K. Lee, and C. S. Ting, *ibid.*, p. 6561.
[26] G. Vignale and K. S. Singwi, *ibid.*, **39**, 2956 (1989).
[27] V. N. Popov, *On the type of Cooper pairing in the high $T_c$ superconductivity*, CERN-TH-5653, 1990.
[28] Z. B. Su, J. Phys. B **70**, 131 (1988).
[29] E. W. Fenton, Phys. Rev. B **40**, 10796 (1989).
[30] Yu. V. Kopaev and A. A. Gorbatsevich, Pis'ma Zh. Eksp. Teor. Fiz. **51**, 327 (1990) [JETP Lett. **51**, 373 (1990)].
[31] A. A. Gorbatsevich, *ibid.*, p. 39. [*ibid.*, p. 46].
[32] G. Vignale and M. R. Heday, Phys. Rev. B **42**, 786 (1990).
[33] P. W. Anderson, Phys. Rev. **86**, 694 (1952).
[34] A. Kampf and J. R. Schrieffer, Phys. Rev. B **41**, 6399 (1990); Phys. Rev. Lett. **62**, 1564 (1989).
[35] B. I. Shraiman and E. D. Siggia, *ibid.*, **40**, 9162 (1982); Phys. Rev. Lett. **62**, 1564 (1989).
[36] C. Jayaprakash, H. R. Krisnamurthy, and S. Sarker, Phys. Rev. B **40**, 2610 (1989).
[37] Z. Y. Weng and C. S. Ting, *ibid.*, **42**, 803 (1990).
[38] Z. Y. Weng, Phys. Rev. Lett. **66**, 2156 (1991).
[39] Z. Y. Weng, C. S. Ting, and T. K. Lee, Phys. Rev. B **41**, 1990 (1990).
[40] T. Giamarchi and C. Lhuillier, *ibid.*, **42**, 10641.
[41] H. J. Schuls, Phys. Rev. Lett. **64**, 1445 (1990).
[42] D. Poilblanc and T. M. Rice, Phys. Rev. B **39**, 9749 (1989).
[43] J. A. Verges, E. Louis, P. S. Lomdahl, F. Guinea, and A. R. Bishop, *ibid.*, **43**, 6099 (1991).
[44] C. I. Kane, P. A. Lee, and N. Read, *ibid.*, **39**, 6880 (1989).
[45] S. R. White, D. J. Scalapino, R. L. Sugar, E. Y. Loh, J. E. Guberratis, and R. T. Scalettar, *ibid.*, **40**, 506.
[46] A. Moreo, D. J. Scalapino, R. L. Sugar, S. R. White, and N. E. Bickers, *ibid.*, **41**, 2313 (1990).
[47] N. E. Bickers, D. J. Scalapino, and S. R. White, Phys. Rev. Lett. **62**, 961 (1989).
[48] N. E. Bickers and S. R. White, Phys. Rev. B **43**, 8044 (1991).
[49] A. Moreo and D. J. Scalapino, *ibid.*, p. 2811.
[50] Yu. A. Izyumov and B. M. Letfulov, Europhys. Lett. 1991 (in press).
[51] Yu. A. Izyumov and B. M. Letfulov, J. Phys.: Condens. Matter **3**, 5373 (1991).
[52] R. O. Zaitsev and V. A. Ivanov, Fiz. Tverd. Tela **29**, 2554 (1987) [Sov. Phys. Solid State **29**, 1475 (1987)].
[53] R. O. Zaitsev and V. A. Ivanov, Physica C **153–155**, 1295 (1988).
[54] N. M. Plakida, V. Yu. Yushankhai, and I. V. Stasyuk, *ibid.* **160**, 80 (1989).
[55] V. I. Belinicher, Zh. Eksp. Teor. Fiz. **98**, 931 (1990) [Sov. Phys. JETP **71**, 519 (1990)].
[56] L. N. Bulaevskii and D. I. Khomskii, Zh. Eksp. Teor. Fiz. **52**, 1603 (1967) [Sov. Phys. JETP **25**, 1067 (1967)].
[57] L. N. Bulaevskiĭ, E. L. Nagev, and D. I. Khomskiĭ, Zh. Eksp. Teor. Fiz. **54**, 1562 (1968) [Sov. Phys. JETP **27**, 836 (1968)].
[58] W. F. Brinkman and T. M. Rice, Phys. Rev. B **2**, 1324 (1970).
[59] I. M. Lifshitz, Adv. Phys. **13**, 483 (1969).
[60] S. Schmitt-Rink, C. M. Varma, and A. E. Ruckenstein, Phys. Rev. Lett. **60**, 2793 (1988).
[61] B. I. Shraiman and E. D. Siggia, *ibid.*, p. 740.
[62] S. A. Trugman, Phys. Rev. B **37**, 1597 (1988).
[63] J. Bonca, P. Prelovsek, and I. Sega, *ibid.*, **39**, 7074 (1989).
[64] J. Bonca, P. Prelovsek and I. Sega, Europhys. Lett. **10**, 87 (1989).
[65] I. Sega and P. Prelovsek, Phys. Rev. B **42**, 892 (1990).
[66] Y. Hasegawa and D. Poilblanc, *ibid.*, **40**, 9035 (1989).
[67] E. Dogotto, A. Moreo, and T. Barnes, *ibid.*, p. 6721.
[68] E. Dagotto, A. Moreo, R. Joynt, S. Bacci, and E. Gagliano, *ibid.*, **41**, 2585 (1990).
[69] Y. Nagaoka, Phys. Rev. **147**, 392 (1966).
[70] E. Dagotto, R. Joynt, A. Moreo, S. Bacci and E. Gagliano, Phys. Rev. B **41**, 9049 (1990).
[71] S. A. Trugman, *ibid.*, p. 892.
[72] S. White, D. Scalapino, R. Sugar, and N. Bickers, Phys. Rev. Lett. **63**, 1523 (1989).
[73] C. X. Chen and H. B. Schuttler, Phys. Rev. B **41**, 8702 (1990).
[74] D. Poilblanc, E. Dagotto, and J. Riera, Phys. Rev. B **43**, 7899 (1991).
[75] W. Stephan and P. Horsch, Phys. Rev. Lett. **66**, 2258 (1991).
[76] J. M. F. Gunn and B. D. Simons, Phys. Rev. B **42**, 4370 (1990).
[77] E. Kaxirax and E. Manousakis, *ibid.*, **38**, 866 (1988).
[78] J. Riera and A. Young, *ibid.*, **39**, 9697 (1989).
[79] K. H. Luk and D. Cox, *ibid.*, **41**, 4456 (1990).
[80] E. Dagotto, J. Riera, and A. P. Young, *ibid.*, **42**, 2347.
[81] M. V. Feĭtel'man, Pis'ma Zh. Eksp. Teor. Fiz. **27**, 462 (1978) [JETP Lett **27**].
[82] L. B. Ioffe, and A. I. Larkin, Phys. Rev. B **37**, 5730 (1988).
[83] V. Emergy, S. Kiveison, and H. Q. Liu, Phys. Rev. Lett. **64**, 475 (1989).
[84] I. E. Dzyaloshinskiĭ, Zh. Eksp. Teor. Fiz. **93**, 1487 (1987) [Sov. Phys. JETP **66**, 848 (1987)].
[85] A. E. Ruckenstein and S. Schmitt–Rink, Intern. J. Mod. Phys. B **1**, 1809 (1989).
[86] A. Parola, S. Sorella, M. Parrinello and E. Tosatti, Phys. Rev. B **43**, 6190 (1991).
[87] L. Chen, C. Bourbonnais, T. Li, and A. M. S. Tremblay, Phys. Rev. B **43**, 6190 (1991).
[88] G. C. Psaltakis and N. Papanicolaou, *ibid.*, **42**, 10952 (1990).
[89] J. Carmelo, M. Dzierzawa, X. Zotos, and D. Baeriswyl, *ibid.*, **43**, 598, (1991).
[90] A. Georges and J. S. Yedidia, *ibid.*, p. 3475.
[91] W. Barford and J. P. Lu, *ibid.*, p. 3540.
[92] N. Kumar, *ibid.*, **42**, 2320 (1990).
[93] A. Auerbach and B. E. Larson, Phys. Rev. Lett. **66**, 2262 (1991).
[94] Z. Y. Weng, C. S. Ting, and T. K. Lee, Phys. Rev. B **43**, 3790 (1991).
[95] M. Uchinami, *ibid.*, **42**, 10178 (1991).
[96] A. Auerbach and B. E. Larson, *ibid.*, **43**, 7800 (1991).
[97] H. Ogato, M. U. Luchini, S. Sorella, and F. F. Assaad, Phys. Rev. Lett. **66**, 2388 (1991).

Translated by S. Chomet